In presenting the dissertation as a partial fulfillment of the requirements for an advanced degree from the Georgia Institute of Technology, I agree that the Library of the Institute shall make it available for inspection and circulation in accordance with its regulations governing materials of this type. I agree that permission to copy from, or to publish from, this dissertation may be granted by the professor under whose direction it was written, or, in his absence, by the Dean of the Graduate Division when such copying or publication is solely for scholarly purposes and does not involve potential financial gain. It is understood that any copying from, or publication of, this dissertation which involves potential financial gain will not be allowed without written permission.

3/17/65
b

ELECTRO-MAGNETIC-FLUX CLUTCHES

FOR SPACE APPLICATIONS

A THESIS

Presented to

The Faculty of the Graduate Division

by

Craig Alan Depken

In Partial Fulfillment

of the Requirements for the Degree

Master of Science in Mechanical Engineering

Georgia Institute of Technology

July, 1966

ELECTRO-MAGNETIC-FLUX CLUTCHES

FOR SPACE APPLICATIONS

Approved:

Chairman

Date approved by Chairman: Sept. 7, 1966

ACKNOWLEDGMENTS

The author wishes to express his most sincere appreciation to his advisor, Dr. Eugene Harrison, for his invaluable guidance, patience and encouragement. Also, to the members of the thesis committee, Dr. Roger P. Webb and Dr. J. Edward Sunderland, goes a heartfelt note of gratitude for their constructive criticism and aid in the preparation of this thesis.

Mr. J. G. Wright, Mr. W. A. Jones, and Mr. R. Anderson are gratefully thanked for their assistance in the design and fabrication of the test apparatus.

The author wishes to thank the clutch manufacturers who willingly donated clutches for testing and clutch information to complete this investigation. Finally, a special note of gratitude is extended to the National Aeronautics and Space Administration for the financial assistance which made this undertaking possible.

TABLE OF CONTENTS

LIST OF TABLES

LIST OF ILLUSTRATIONS

Figure Page

Figure Page

NOMENCLATURE

A	area, $in.^2$
B_{avg}	average flux density, $lines/in.^2$
b	constant
C	electrical capacitance, farads
C_p	heat capacitance, $Btu/lb-^oF$
C_1	Planck constant, 1.1870×10^4 $^4/ft^2/hr$
C_2	Planck constant, 2.5896×10^4 $-^oR$
E	voltage, v
E_g	gray-body emissive power, Btu/ft^2-^oR
e	Napierian base, 2.71828.....
$\exp(y)$	Napierian base to the power (y)
F_{1-2}	shape factor from object 1 to object 2
f	co-efficient of kinetic friction
H_{2max}	hysteresis coercive force, ampere-turns/in.
h	convective heat transfer co-efficient
I	current, amperes
I_q	quiescent current level, amperes
I_{ss}	steady-state current level, amperes
J_L	mass moment of inertia, $in.-lb-sec^2$
K	constant
k	constant

L	electrical inductance, henry axial length, in.
ln	Napierian logarithm
N_{max}	maximum cyclic frequency, cycles/unit time
n	constant
P	number of magnetic poles
Q	thermal energy transfer, Btu/hr
Q_c	conductive heat transfer, Btu/hr
q	energy transfer, Btu/hr-ft^2
R	electrical resistance, ohms thermal resistance, hr-^{o}F/Btu radius, in.
R_a	effective reluctance of "a," 1/henry
R_g	effective reluctance of gap and powder, 1/henry
s	Laplace operator
T	torque, in.-lb
T_e	eddy-current coupling torque, in.-lb
T_h	hysteresis coupling torque, in.-lb
T_{ss}	steady-state torque level, in.-lb
T	thermal temperature, degrees Rankine, ^{o}R
T^{o}	thermal temperature, degrees Fahrenheit, ^{o}F
t	time, seconds, sec radial thickness, in.
t_s	time to reach steady-state, sec
V	volume, in.^{3}

W_d	energy, Btu or ft-lb
W_h	hysteresis energy loss, joules/in.^{3}/cycle
w	weight, pounds, lb
α_T	temperature correction factor
α_t	time correction factor
ϵ_g	gray-body emissivity
ϵ_i	radiant emissivity of surface "i"
$\epsilon(\lambda)$	monochromatic emissivity
λ	wavelength of radiant emission, microns, pole pitch, in.
π	constant, 3.14159.....
ρ	resistivity per unit volume, ohms/in.^{3}
ρ_i	radiant reflectivity of surface "i"
σ	Stefan-Boltzman constant, 0.1714 x 10^{-8} Btu/hr-ft^2-$^\circ$R
τ	time constant, sec
φ	magnetic flux, webers
ω_i	rotational velocity of shaft "i," rpm

SUMMARY

The objective of this study was to determine the capabilities, limitations and operating characteristics of electro-magnetic flux clutches in order to evaluate their effectiveness in a space vehicle application.

In order to accomplish this goal, clutch manufacturers were asked to supply data for a survey to determine the types of clutches available. From these data, several clutches were selected as characteristic of the industry and were obtained for the purpose of laboratory testing. In addition, a survey was made of the current technical literature concerning electro-magnetic flux clutches and clutch couplings.

From the literature survey, a complete discussion is given on the operating characteristics of the three different electro-magnetic flux clutches. Experimental tests, devised to supplement this information, showed the magnetic particle clutch as being susceptible to change in particle distribution. Also, the torque time response was found to be a non-linear function of the coil current and slip-speed. A high temperature test showed the coil resistance to increase with

temperature. However, despite the inference in the literature that this increase in coil resistance was capable of protecting the clutch from over-heating, this was not found to be true. Similar tests were performed on a hysteresis clutch showing it to conform closely to the published characteristics.

A summary of the analytical and empirical mathematical relationships available to describe clutch performance is included. Equations are given relating steady-state torque level to the steady-state current level and the torque as a function of time to the coil flux for a magnetic-particle clutch, as well as a transfer function relating flux to coil current. Semi-empirical equations for hysteresis and eddy-current torque are presented.

A survey was made of the physical and performance characteristics of commercially available clutches on the basis of clutch vendor literature. Various performance indices were calculated. These showed electro-magnetic flux clutches have a torque to weight ratio as great as 23.0 (in.-lb/lb); a torque to volume ratio as great as 1242×10^4 (in.-lb/in.-lb-sec^2); and a linear power gain in excess of 1900 (watt/watt).

Finally, an energy analysis was made in order to determine the maximum amount of energy any particular clutch

is capable of dissipating. A general expression for the energy developed in a single clutch cycle is given. A discussion is included regarding the means of dissipating energy through the various modes of heat transfer. Equations for the radiant heat transfer from the clutch to its surroundings are presented, and possible improvements are suggested.

CHAPTER I

INTRODUCTION AND HISTORICAL BACKGROUND

Clutches have long been used as a convenient means of connecting a power-driven shaft with a load carrying shaft. The most common clutches are mechanical contact, fluid and electro-magnetic flux devices. The purpose of this work is to investigate electro-magnetic flux devices.*

From a historical standpoint the induction clutch coupling, commonly called an eddy-current clutch coupling, was the first electro-magnetic clutch (E.M.C.) to be developed. The initial work on the particle clutch was accomplished in 1948 by J. Rabinow (3), of the United States National Bureau of Standards. As a result of its slow evolution through industrial research, the hysteresis clutch has only recently found widespread use.

The search for applications of the various types of electro-magnetic flux clutches and couplings has led to a great many varied and interesting mechanisms. It is, therefore, reasonable to expect that the electro-magnetic flux

---

*See R. I. Anderson (1) and W. A. Jones for discussions of mechanical contact clutches and fluid couplings, respectively.

clutch has been and is being considered for various space-oriented applications.

Objective

The objective of this work is to compile information about the various types of electro-magnetic flux clutches and couplings commercially available, and forecast their usefulness in a space application. To accomplish this end the author has surveyed the clutch manufacturers and read the current literature to obtain data for the comparison of the various magnetic flux clutches. In addition, several clutches were selected as representative of the industrial types and were subjected to laboratory testing. It should be noted, however, that the clutches selected for testing were not necessarily designed for space applications. It is hoped, however, that an extrapolation of the data obtained for a clutch or clutch coupling may be useful in designing for space use.

Types of Clutches Investigated

There are basically three types of electro-magnetic flux clutch couplings. These are the eddy-current clutch coupling, the hysteresis clutch and the magnetic-particle clutch. All three types of devices have found well-defined

areas of application.

A distinction should be made between a clutch coupling and a clutch. The literature usually designates a clutch as a load-carrying coupling capable of total disengagement of input and output shafts and the total engagement of the input and output shafts. The clutch coupling differs by not having the capability of total engagement, i.e. non-slip operation.

The eddy-current or induction device is a clutch coupling since it is not capable of non-slip operation. The reason for this continuous slippage operation will be explained later in this chapter.

The eddy-current clutch coupling has found widespread application in heavy-duty velocity control systems. A typical application is that of a diesel railroad locomotive. Here, the diesel engine drives a d.c. generator whose output is then used to drive the electric drive-wheel motors. For reasons of efficiency, it is best to maintain the diesel engine's speed relatively constant. This in turn produces a constant generator output power. In order to control the operating speed of the motor a large shunting resistor would be required to change the power input to the motor. This would certainly reduce the overall operating efficiency of

the system. However, the introduction of an eddy-current clutch-coupling between the drive motor and the drive wheels eliminates the need for the inefficient shunting resistor. Also, this mode of operation allows an extremely easy control of locomotive speed.

The transmitted power for a standard eddy-current clutch coupling may range from one horsepower to one-hundred and twenty-five horsepower. And, specially designed units may transmit even greater amounts of power. The most salient characteristic of the eddy-current clutch coupling is that its transmitted torque is directly proportional to both its slip speed and control current.

The hysteresis clutch is a true clutch in that it is not necessary for the device to operate in continuous slip. It is usually applied in the same type of application as the eddy-current clutch. However, because its bulk increases greatly as the power to be transmitted, it is usually limited to an intermediate power range, that is, less than one horsepower.

The hysteresis clutch is characterized by an extremely smooth operation, a near-linear torque variation with control current, no wear or in-service adjustments, and a very stable torque control.

The hysteresis clutch finds wide-spread application when an extremely smooth actuation cycle is required and/or the power to be transmitted is beyond that of the magnetic-particle clutch but not in excess of about one horsepower (746 watts).

J. Winston (4) discusses the application of the hysteresis clutch to an high-power positioning servo system. This requires that the displacement of the controlled variable be completely reversible in any given operating interval. In order that the drive motor operate at a constant velocity, the clutches must be arranged in a so-called "push-pull" configuration. This arrangement is indicated in Figure 1. It is evident, however, that this arrangement requires that for continuous control one of the clutches must always be operating in slip. This condition is not objectionable as long as the energy dissipated does not raise the temperature of the system above that for which the electrical wire insulation will break down.

Figure 2 shows a typical velocity feedback positioning servo as discussed by Winston in reference (4).

The magnetic-particle clutch finds application in similar types of systems as the hysteresis clutch. However, its transmitted power is, in general, much less than that of

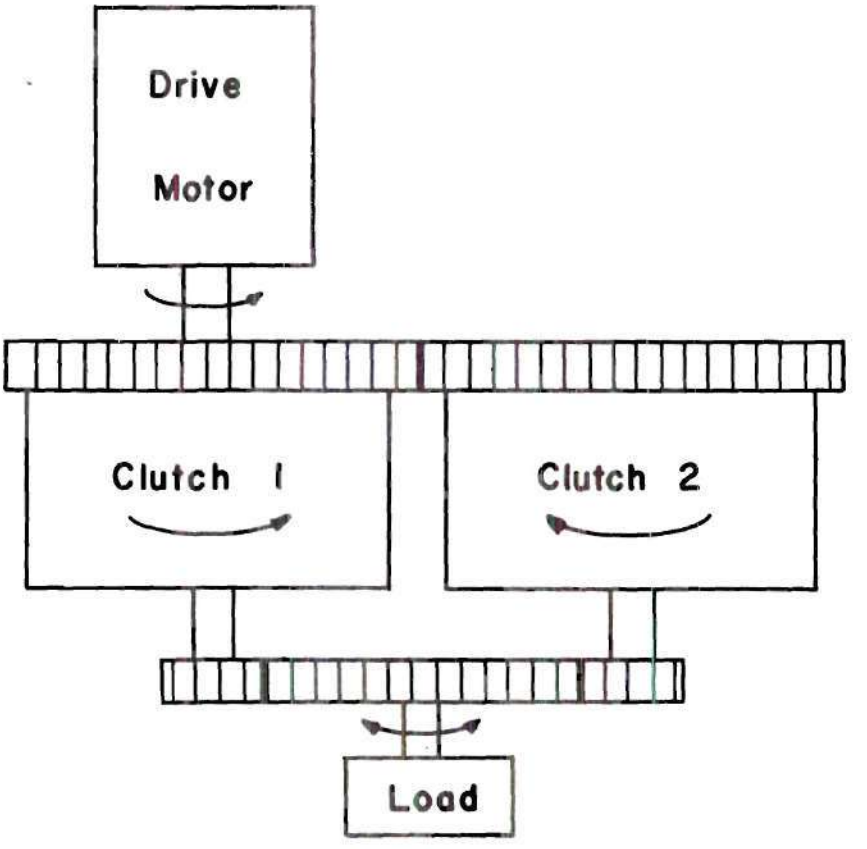

Figure 1. Two Clutches in Push-Pull Arrangement

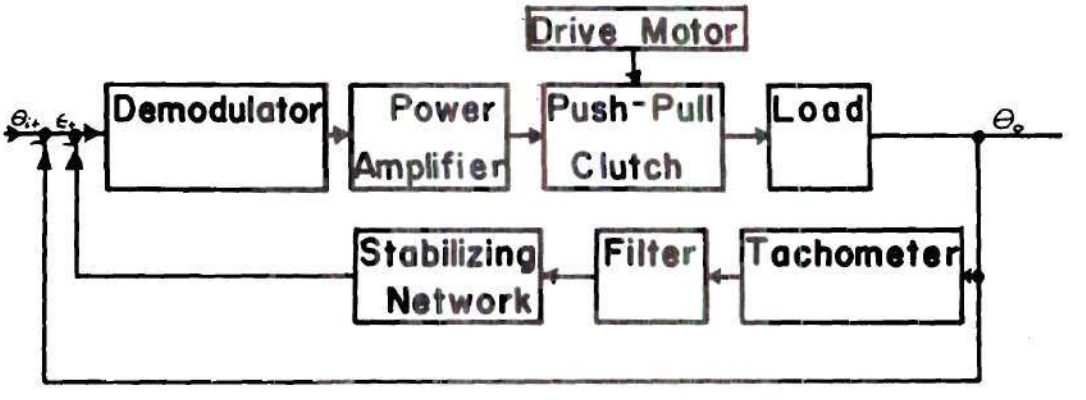

Figure 2. Block Diagram of Positioning Servo with Push-Pull Clutch Arrangement

the hysteresis device.

The particle clutch has operating characteristics similar to those of the hysteresis clutch except that it is usually smaller in physical size, has a somewhat faster response time, and displays less linearity and smoothness in its actuation.

Means of Operation

All electro-magnetic flux clutches are similar in their basic means of operation. That is, all flux clutches use an electrical current to produce an electro-magnetic field. Torque is produced by some interaction of this force field with its surroundings. The different means of interaction produce three basic types of electro-magnetic clutches and clutch-couplings.

Each of the electro-magnetic devices has three basic components: namely, an input rotor, a current-carrying coil and an output rotor. In general, the input rotor is of high inertia and the output of low inertia. The coil may be attached to, and hence rotate with, the input rotor or may be stationary.

If the coil is attached to the rotor, slip rings are required to transmit current to the coil. The advantage of the stationary coil is that no such slip rings are required.

However, in the case of the stationary coil the field produced in the rotor for a given current is less than that of the rotary coil. Since the torque transmitted is directly proportional to the field in the input rotor, the relative configuration might be of consequence in any particular design application.

As previously stated, the eddy-current clutch coupling operates in continuous slip. The basic configuration of the eddy-current clutch coupling is shown in Figure 3.

When the current-carrying coil is energized a magnetic field is set up in the multi-pole rotor as shown in the diagram. Since the air gaps between input and output rotors are small as compared to that between the pole pieces, all the magnetic flux from the poles on one end of the coil is magnetically connected through the output rotor to the poles on the other end of the coil. Hence, a complete magnetic circuit is accomplished from the input to the output rotor and back to the input rotor. The flux in the output rotor is concentrated immediately opposite the poles of the input rotor. Therefore, if there is any relative motion between the two rotors the line of travel of the flux concentration remains opposite the input rotor poles. As the flux concentrations move circumferentially through the output rotor,

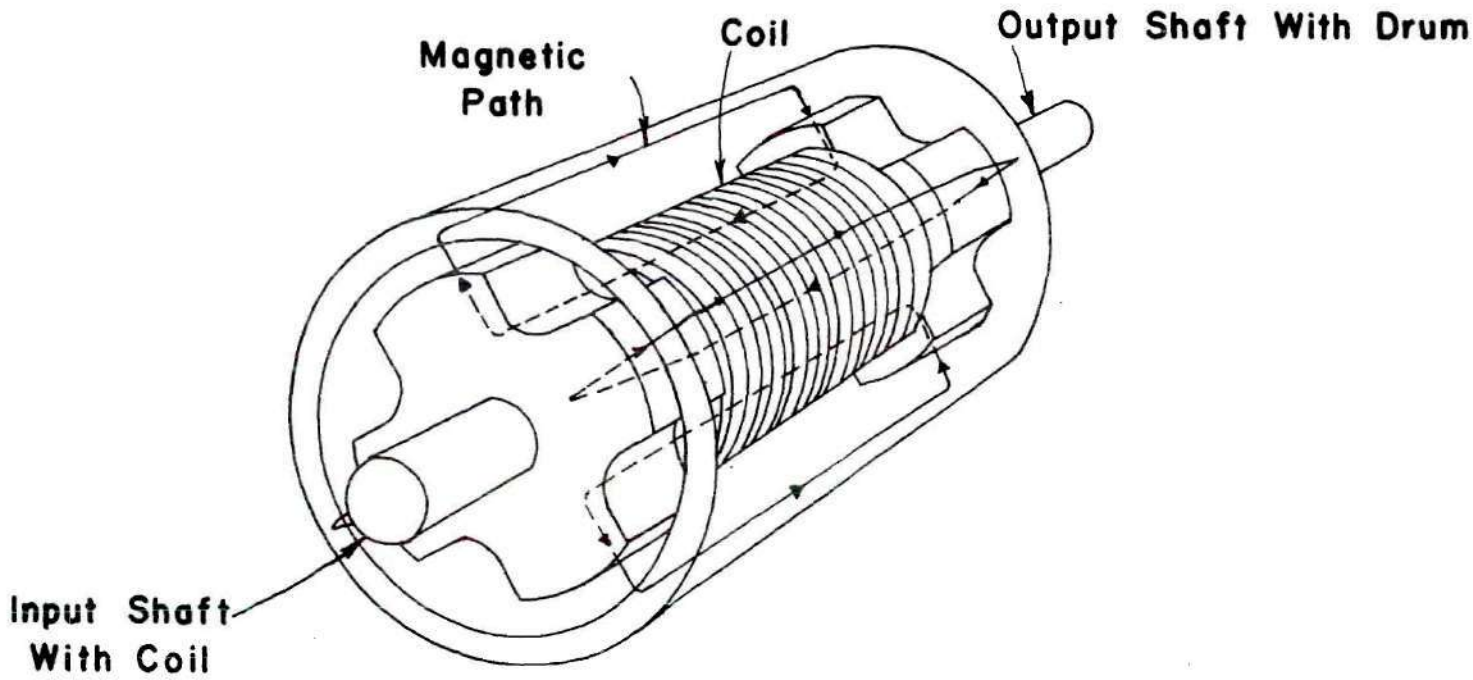

Figure 3. Typical Eddy-current Clutch Coupling Configuration

eddy-currents are induced in the output rotor itself. These currents in turn produce secondary magnetic fields which oppose those originally produced by the coil current. The interaction of the two fields produces a torque in the output rotor which tends to rotate it in the same direction as that of the input rotor (5).

There is no uniqueness as to designation of input or output shafts. If the so-called output shaft were the driven shaft, then the remaining shaft would tend to follow in the same manner as previously described. However, since the clutch coupling usually has the task of accelerating the driven member, it is most economical to have the input of the clutch coupling be the rotor with the largest inertia. If the device has a rotary coil then the input shaft should be as noted in Figure 3.

If the device has a stationary coil the coil is physically located within the input rotor. Hence, there is necessarily an air gap between the coil and its core and the input rotor. This additional air gap necessarily reduces the flux concentration in the driven rotor resulting in a reduced torque.

A typical cross-sectional drawing of an hysteresis clutch is shown in Figure 4. This diagram shows the three

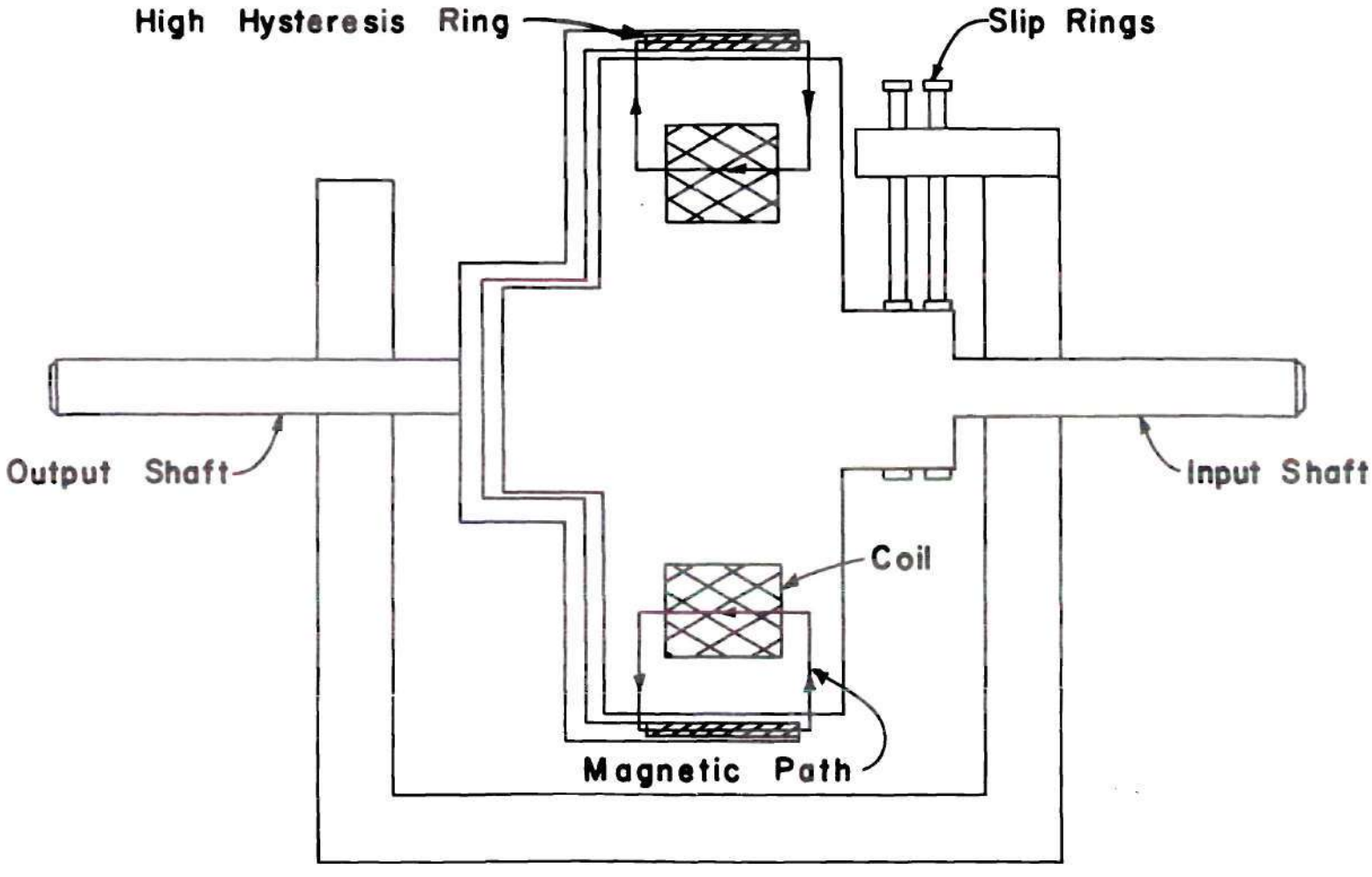

Figure 4. Typical Hysteresis Clutch

basic components of an electro-magnetic flux device; the input rotor, coil and output rotor. As with the eddy-current clutch coupling the coil is usually wound upon the input shaft. The output rotor is actually cup-shaped and has the added feature of an high hysteresis metal ring pressed into it and placed opposite the coil.

When the coil is energized the magnetic flux path created passes through the ring in a manner similar to the eddy-current device. However, unlike the situation in the eddy-current device, relative motion between the input and output shafts is not required to transmit torque.

Figure 5(a) shows a schematic of the hysteresis ring in the field of the coil. Since the magnetic field may be considered a vector quantity, the minute arrows in the ring indicate the direction of the flux in each indicated segment of the ring.

In Figure 6 the solid line curve is the average magnetization curve. As each segment of the ring rotates through 360° with respect to the coil, its magnetic state may be indicated on this average curve. A segment of ring at point A in Figure 5(a) has an initial magnetic state corresponding to point (e) on Figure 6. As the segment is rotated to point B the flux density increases to a maximum at

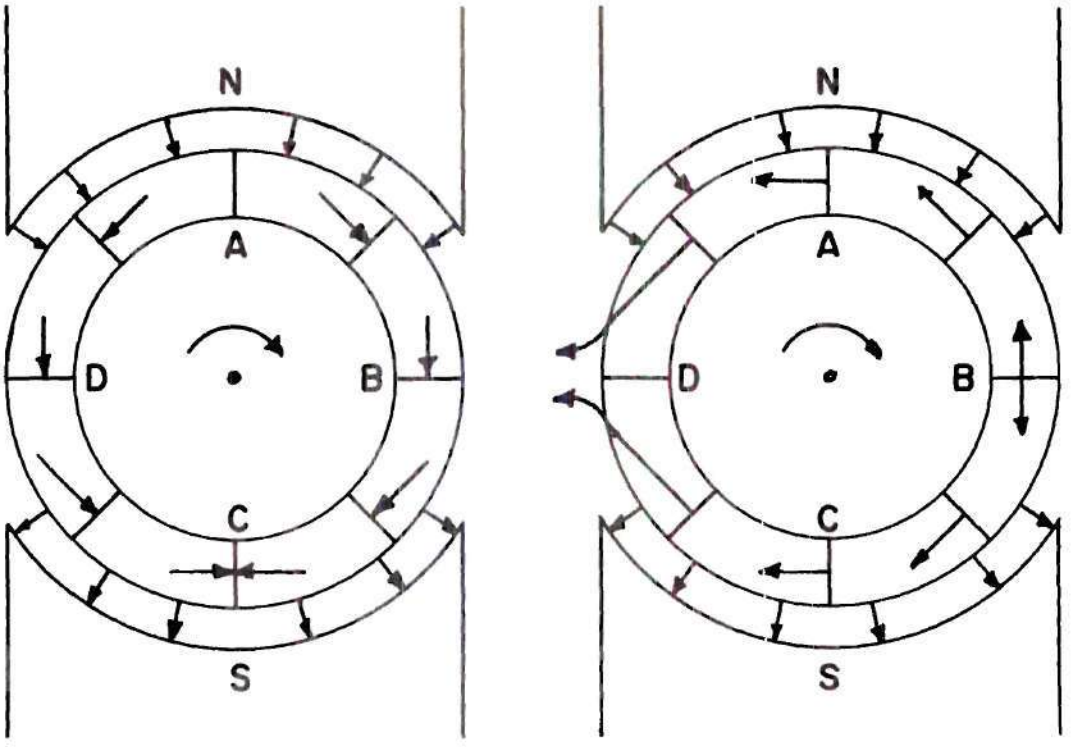

a) Along Average Magnetization Curve

b) Hysteresis Components

Figure 5. Magnetic Field Strength Distribution in the Hysteresis Ring

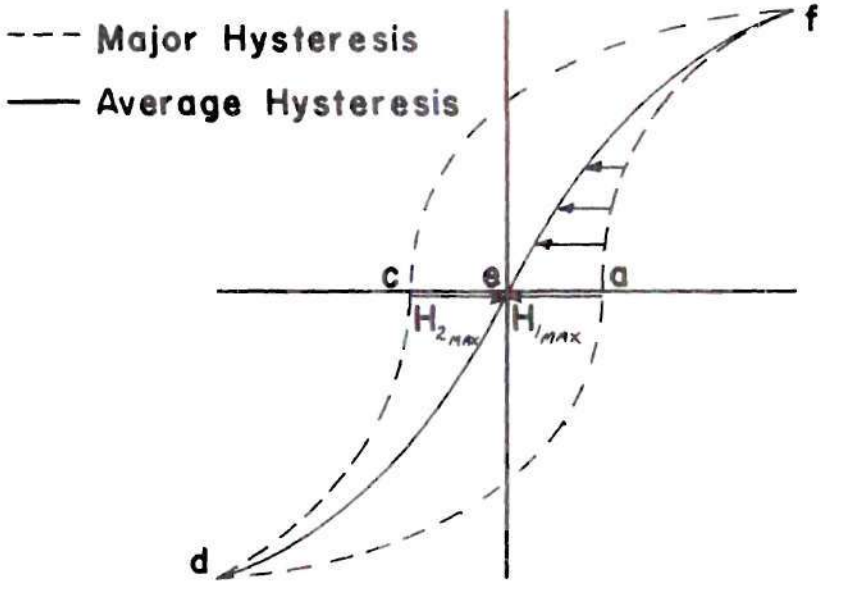

Figure 6. Average Magnetization Curve and Major Hysteresis Curves

point (f). Rotating the segment to points C, D, and returning to A allows the segment to have a flux density corresponding to points (e), (f) and (e), respectively.

Torque can be produced between the rotating magnetic field and the rotating ring only when the direction of the vectorial sum of the flux in the coil segments is different than that of the coil itself. Figure 5(a) shows that operation along the average magnetization curve produces a net flux in the ring in exactly the same direction as the coil field, and therefore, no torque is produced.

The ring is constructed of some high hysteresis material such as hardened cobalt steel. The hysteresis components of the flux, however, allow the direction of net flux in the ring to be mis-aligned with the coil. Referring now to Figure 5(b) and the dotted curve in Figure 6, the magnetic state of the ring segments may again be traced through a complete revolution with respect to the coils.

At point A on the ring the magnitude of the flux is H_{lmax} and indicated as such in Figure 6. As the segment rotates to point B the field strength diminishes. During this phase of the rotation, the major hysteresis curve in Figure 6 has been traversed from points (a) to (f). As the ring segments arrive at point C the strength of the field is again

a minimum and returns to its original maximum at point A. This corresponds to traversing the hysteresis curve from (f) to (c) to (d) and returning to (a).

Referring to Figure 5(b), it is possible to see the axis of the magnetic flux in the ring is in quadrature with that of the coil. Such a combination of fields will produce a torque between the coil and the ring.

The strength of the induced pole in the ring, and hence the transmitted torque, is a function only of the area enclosed by the major hysteresis curve in Figure 6. This pole strength is completely independent of the relative speed between the ring and the coil.

A complete discussion of the means of operation of the hysteresis clutch may be found in references (4) and (6) of the Bibliography.

The electro-magnetic particle clutch differs from the eddy-current and hysteresis devices in that there is a physical working medium in contact with both the input and output rotors.

Figure 7 shows a typical particle clutch cross-section. Again the three basic components are present. In most cases, the coil is an integral part of the input rotor. However, as in the other types of clutches the coils may be

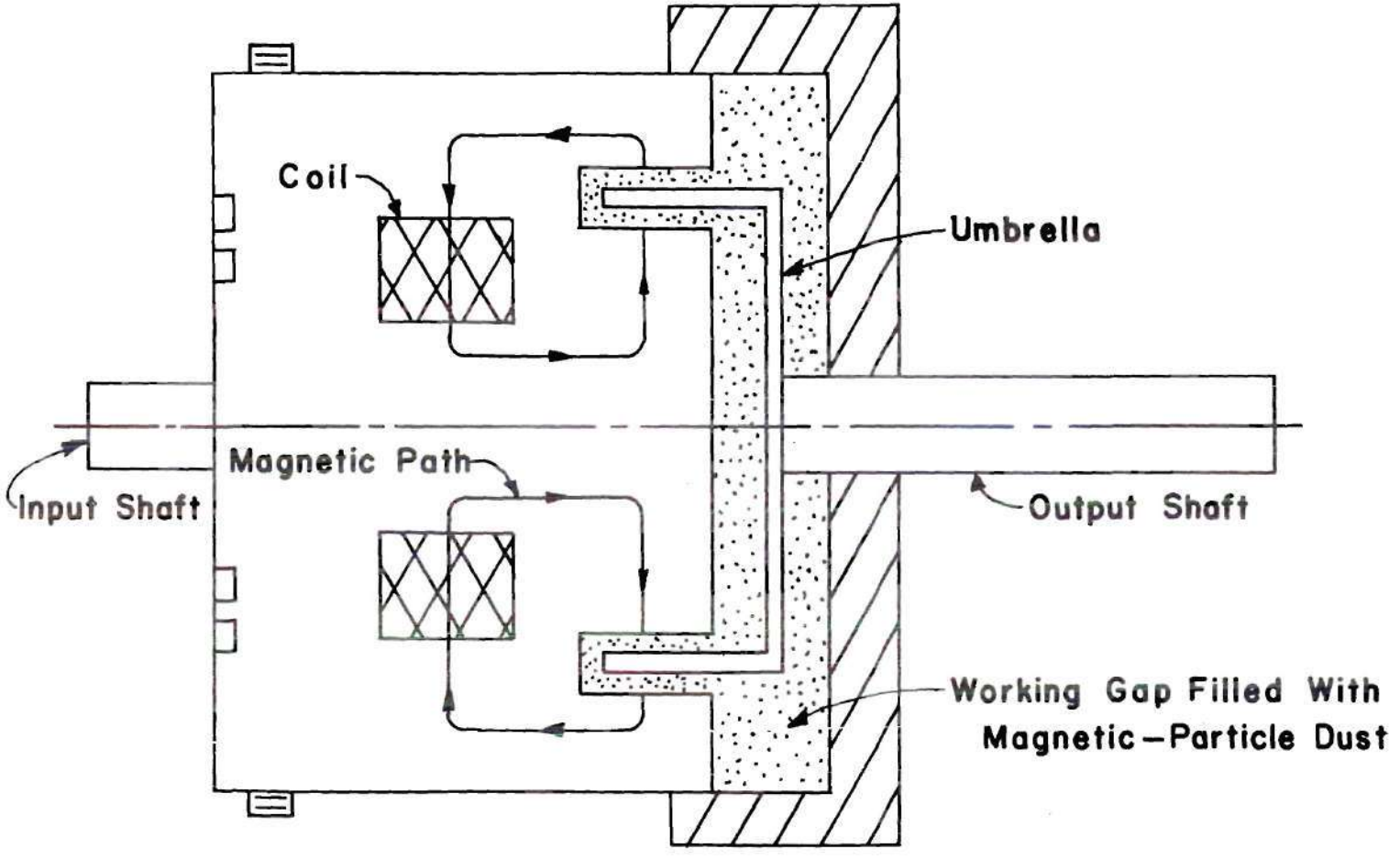

Figure 7. Typical Magnetic-Particle Clutch

stationary but only with a corresponding decrease in the maximum transmitted torque.

The clutch operates on a very simple principle. When the coils are energized the magnetic flux path traverses the air gap which contains a fine metallic powder and the lip of the output rotor or umbrella. The field itself magnetizes the individual particles and causes the particles to form into chains spanning the gap and touching both input and output rotors. Naturally, these particles exert a force on both the input rotor and umbrella. Therefore, if there is any torque to be transmitted the static friction between the rotor and the particles themselves and the output umbrella allows this torque to be transmitted from one shaft to the other. If there is slippage between the input and output shafts the kinetic friction between particles and rotors becomes the torque-producing agent, (3), (7), (8).

Additional Literature

The Bibliography shows a number of references not directly used in this work. These are a very few of the great numbers of articles appearing in the literature concerning the application of electro-magnetic clutches and clutch couplings to new and varied areas. However, several authors and publications should be mentioned.

The most basic portion of any work involving clutches and their use is a thorough understanding of how past designers have used the various clutches and clutch couplings in their designs. For this reason several articles are here cited, not necessarily because they deal with electro-magnetic flux devices, but rather because they deal with the classical approaches to designing a clutching system.

Reference (9) is an article presented as a survey of the technical "know-how" of clutch engineering. Although written in 1952 the essence of the article is completely contemporary. However, caution should be observed in the use of the numerical data presented, as it is not a true indication of present-day production equipment.

Reference (10) discusses the use of an electrically-actuated friction clutch to an off-on-modulated reversing clutch servo system. Although the magnetic-particle clutch was not an applicable device for this system when the article was written in 1953, recent designs for the particle clutch have all but completely eliminated the friction clutch from this type system.

References (11), (12), and (13) are included as additional guides to present-day use of all types of clutches in actual systems.

All three types of electro-magnetic flux devices are characterized by their lack of wearing parts when operated in continuous slip. This allows their use in systems in which amounts of mechanical energy must be removed from the system for periods of time.

As a result of the direct dependence of transmitted torque on clutch coil excitation it is possible to use the electro-magnetic clutch as a torque-limiting device. Applications in this manner might include winding and wrapping operations on a production line.

The Russians as reported by Vorb'yeva, (7), have done a great deal of work on both analytical and empirical investigations of electro-magnetic flux devices. Vorb'yeva presents a series of cut-away drawings showing a great number of the possible configurations for magnetic-particle clutches. Indeed, several of these designs are currently used in the United States. However, several are unique and may possibly improve clutch performance in any given specific application. Figure 8 is a reproduction of the configuration design flow-chart as presented by Vorb'yeva,(7), page 62. This chart and its accompanying clutch cross-sectional drawings, systematically organize the search for useful clutch configuration design studies.

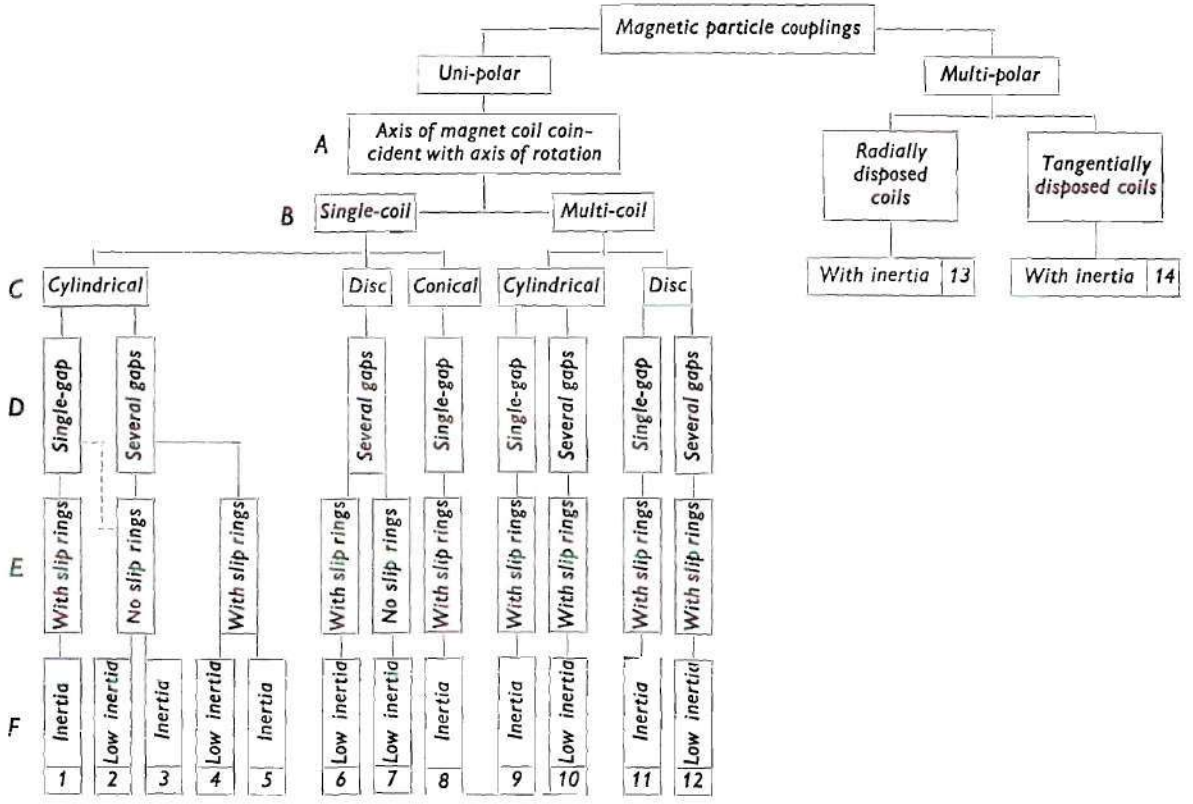

Figure 8. Classification of Possible Magnetic-Particle Clutch Configurations (after Vorob'yeva)

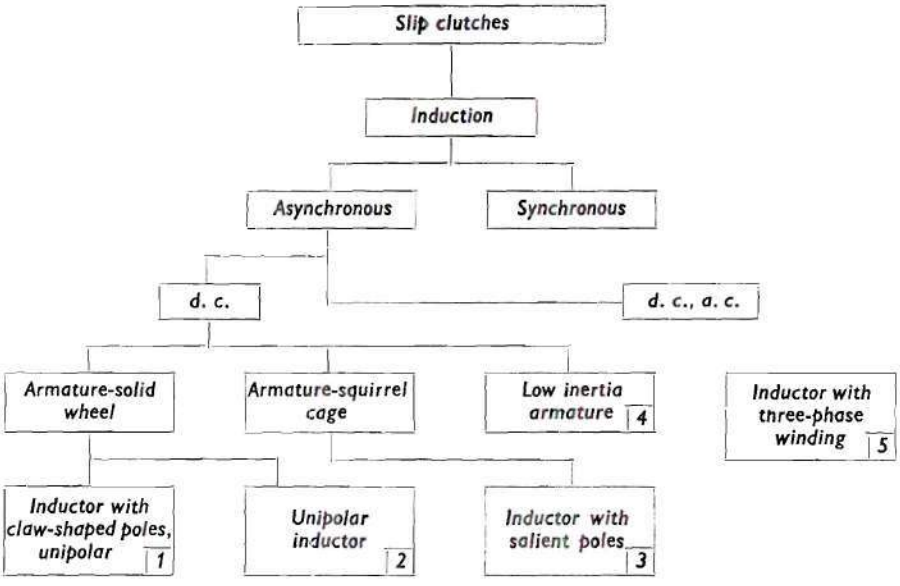

Figure 9. Classification of Possible Hysteresis and Induction Clutch Configurations (after Vorob'yeva)

Vorb'yeva presents another configuration design flow-chart dealing with the induction clutch coupling and the hysteresis clutch. This flow-chart is reproduced in Figure 9. It should be noted that the Russians refer to an eddy-current clutch coupling as an "asynchronous induction slip-clutch." Also, the hysteresis device is referred to as a "synchronous induction slip-clutch." The Russian nomenclature has been preserved in Figure 9. Also, included in the discussion (reference 14) are several cut-away drawings of the designs classified in Figure 9.

Additional application and design information on the eddy-current and hysteresis devices may be obtained from references (4), (15), and (16).

Additional references for the application and design of the magnetic particle clutches are given in the Bibliography, (17) through (27).

CHAPTER II

EXPERIMENTAL INVESTIGATION

Purpose of Investigation

The purpose of the experimental investigation was to obtain the necessary data to accomplish the particular objectives mentioned in Chapter I.

Specifically, information was desired as to the direct dependence of the transmitted torque on the coil control current. Also, in order to aid the designer, it was felt that the time history of the transmitted torque should be documented. In general, the clutches were tested to see if the torque or time response is seriously affected by any particular condition of application.

After collecting the experimental data, a comparison was made with current vendor clutch specifications. Company names will be associated with particular clutches only for the purpose of identification. No attempt is made to compare or rate clutches according to their manufacturers. The result of the investigation and comparison should allow the designer to compare the clutch types as to their possible application in any design, in particular, with respect

to applications in a space environment.

Tests and Experimental Equipment

Basically, two tests were performed on each clutch. The first was to determine the torque dependence upon coil current in a static condition. The second was to determine the torque and current time history at various current levels and at various values of initial slip speed.

Figure 10 shows a sketch of the test apparatus arrangement used to determine the static torque versus coil current characteristics. The general procedure was as follows. The clutch was energized by a given constant coil current. The corresponding torque capability of the clutch was found by slowly loading the water weight. The torque at which the clutch slipped was considered its torque capability. The results of these tests will be discussed in Chapter III.

The second series of tests were performed to determine torque time histories of each clutch using the test apparatus shown in block diagram form in Figure 11. This system employs a feedback control to maintain a near constant clutch input shaft velocity during testing. The central source of power is a hydraulic power supply. This feeds a hydraulic motor through an electrically controlled servo-valve. Feed-

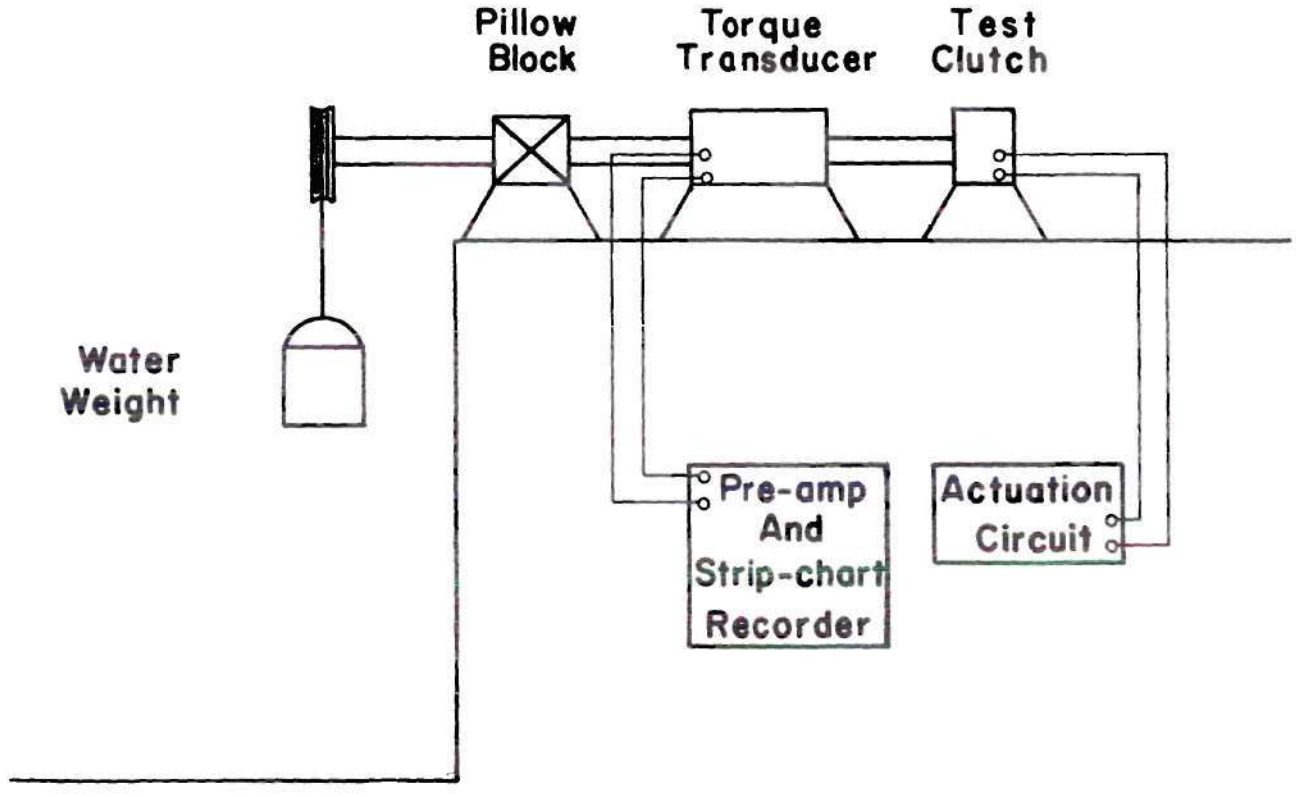

Figure 10. Static Torque vs. Current Test Apparatus

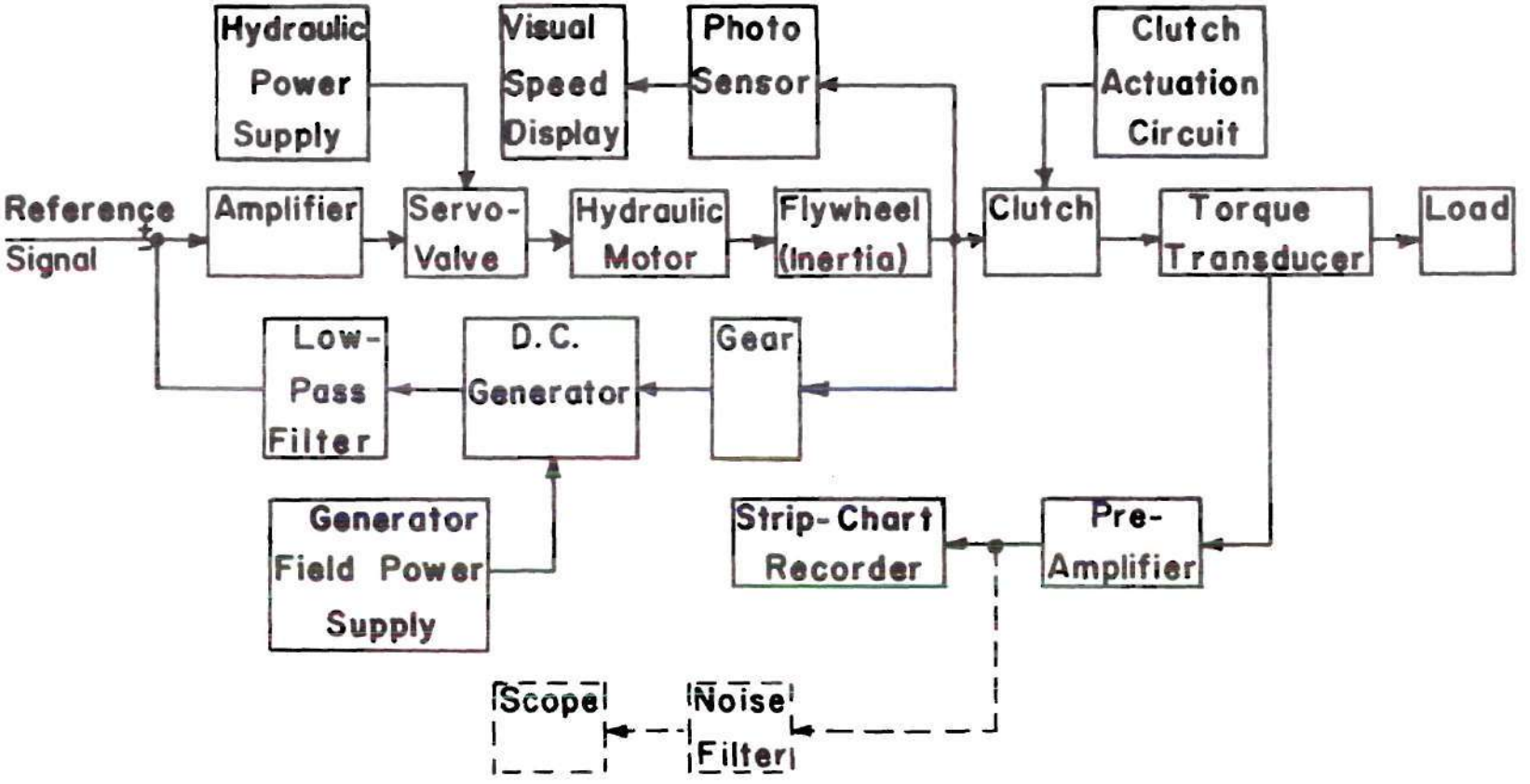

Figure 11. Block Diagram of Experimental System

back is supplied by a d.c. generator geared to the input shaft of the clutch to be tested. For reasons of stability the output of the feedback generator was passed through a "low-pass" filter before entering the summing circuit. The control error was fed through a d.c. amplifier to the servo-valve. The flywheel serves to aid in maintaining input speed at a near constant level while the clutch itself is being activated.

Clutches normally drive some type of inertial load. However, it has been noted that the torque characteristics of the clutch are the same regardless of the size of the load inertia.* Hence, the output shaft was rigidly secured to simulate an infinite load inertia, totally eliminating any motion of the output rotor of the clutch.

A visual check was maintained on the velocity of the clutch input shaft. This was accomplished by counting, with a digital counter, signals produced by a photo-sensitive monitor placed adjacent to the teeth of a polished gear on the clutch shaft.

The torque produced by the test clutch was monitored by a torque transducer placed in line between the clutch and the rigidly-secured shaft (i.e., infinite load inertia).

*See R. I. Anderson, (1), pp. 11-12.

The torque transducer's signal was amplified prior to permanent recording on either the strip-chart recorder or the memory scope. Because of the extreme sensitivity of the scope, a noise filter was placed between the pre-amplifier and the scope. Because of the relatively slow rise time of the electro-magnetic flux clutches tested, satisfactory results were obtained with the strip-chart recorder. A detailed description of the test apparatus is given in Appendix A.

At a fixed current level the clutch was activated with a slip-speed of 300 revolutions per minute (rpm). The actuation was repeated several times to insure a reproducible result. Then using the same coil-current level the test was repeated for slip speeds of 650 and 1000 revolutions per minute. The torque time histories for these tests were collected using the strip-chart recorder as discussed earlier.

The torque time history was then investigated to determine its dependence upon the magnitude of the initiation current. Here a slip-speed of 1000 revolutions per minute was maintained while clutch actuation took place for at least three different current levels. The magnitudes of current varied from clutch to clutch. This was a result of

Table 1. Test Clutches and Tests Performed

Clutch	Static-Torque vs. Current	Static-Torque Temperature	Torque time history w.r.t. slip-speed	Torque time history w.r.t. current level	Current Time History	Torque time history w/special activation circuit
D-4	X		X	X	X	X
I-4	X		X	X	X	
I-5	X	X	X	X	X	X
I-8	X		X	X	X	

the varying current requirements of each clutch.

A special actuation circuit was built for the purpose of improving the time response of clutch engagement. The characteristics of this circuit will be discussed in the next section of this chapter.

The test procedure involved operating the clutch at a slip-speed of 1000 revolutions per minute and then actuating the clutch with the special circuit. As before, the actuation was repeated several times to insure a consistent result.

One additional test was performed, although it was confined to one magnetic-particle clutch. This was a test to determine the torque characteristics of the clutch as its internal temperature increased. The discussion of this test will be left for a later section of this chapter.

Table 1 shows a listing of the clutches tested and indicates what tests were performed on each clutch. All clutches did not undergo all the tests devised. The reason for this seeming incompleteness was either the fact that the clutch could not be adapted to the test or that the performance of the test would not produce additional useful data.

Actuation Circuits

One important characteristic of a clutch system is

the length of time required for full activation of the torque carrying device. In all electro-magnetic flux devices, the torque transmitted depends directly upon the current in the coil. It is therefore evident that during any given activation a more rapid response will be obtained if the coil current is brought to its operational level as rapidly as possible.

If the time constraint of a system cannot be met by clutch over-design then the only alternative is to devise an electrical forcing circuit to decrease the response time. Saliatesta (27) discusses several means of reducing the time required for both a torque build-up and torque tear-down. Figure 12 shows several of these suggested circuits.

Figure 12(a) is a diagram of a normal activation circuit. The clutch is shown to be constructed of an inductance L_C and an internal series resistance R_C. It is assumed that these clutch characteristics are constant throughout the clutch operation. The resistance R is simply a current-limiting device.

When the switch in Figure 12(a) is closed, the current in the coil builds up according to the equation

$$I = \frac{E}{R + R_C} (1 - e^{-t/\tau}) \qquad (2.1)$$

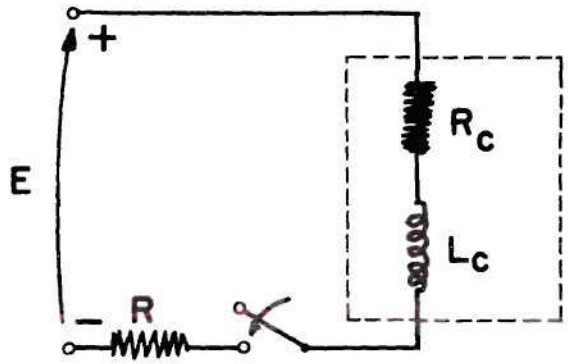

a) Normal Clutch Activation

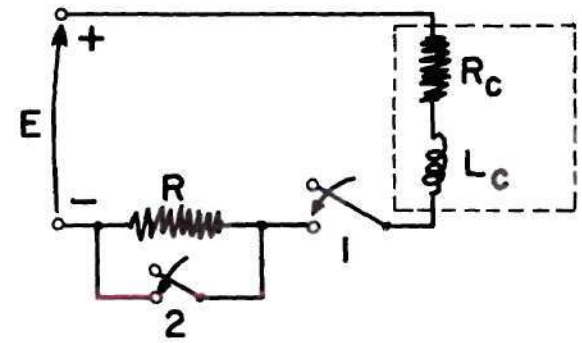

b) Double Switch Circuit

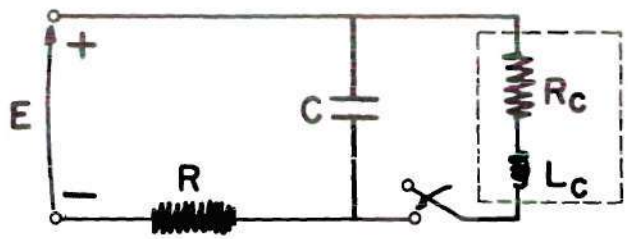

c) Capacitor Supply

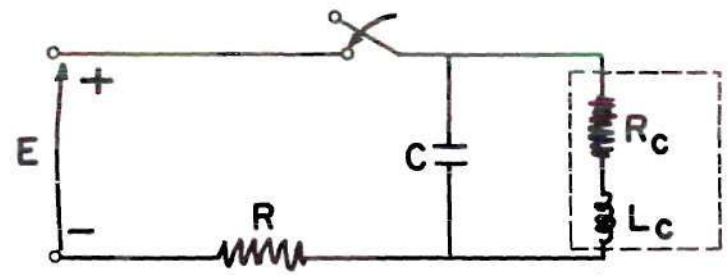

d) Shunting Capacitor

Figure 12. Passive Clutch Activation Circuits

where

$$\tau = \frac{L_C}{R + R_C} \qquad (2.2)$$

After approximately 4τ seconds the steady-state or operational current-level in the clutch is

$$I = \frac{E}{R + R_C} \qquad (2.3)$$

It is evident from (2.2) that the time required to attain the normal operating current can be decreased simply by making the resistance R large. This, however, usually requires an increase in the source voltage E to maintain the steady-state current, which may prove to be inconvenient.

The circuit in Figure 12(b) shows the addition of a shunting switch across the resistance R. This switch is maintained in a closed position until the current I in the clutch has attained the desired level given by equation (2.3).

The circuit in Figure 12(c) is designed to deliver a high capacitor discharge to the clutch when the switch is closed. Figure 12(d) shows a capacitor circuit which aids the decay of current in the clutch. In both of these circuits the capacitors should be chosen such that the decay or build-up of current will satisfy the necessary time constraint.

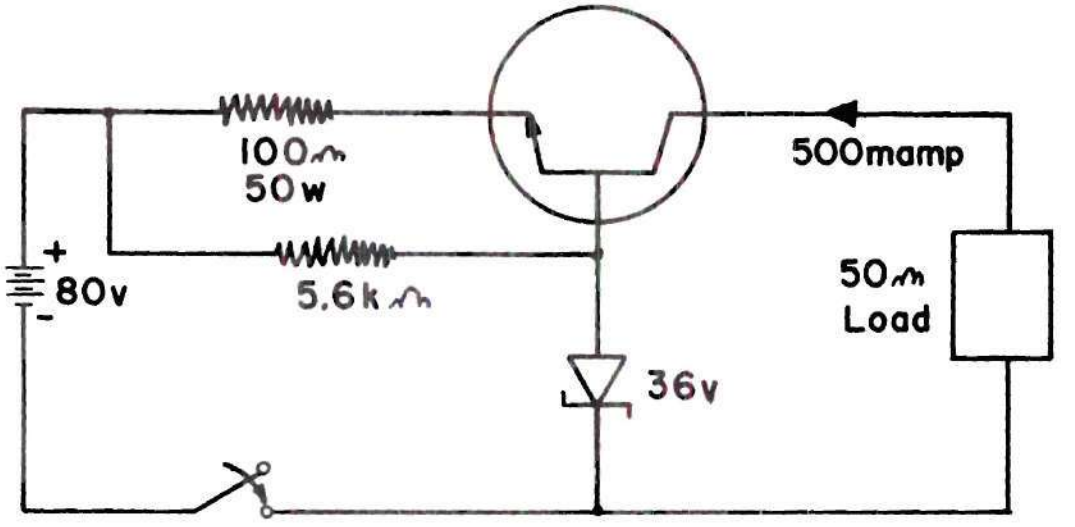

Figure 13. Solid-state Activation Circuit

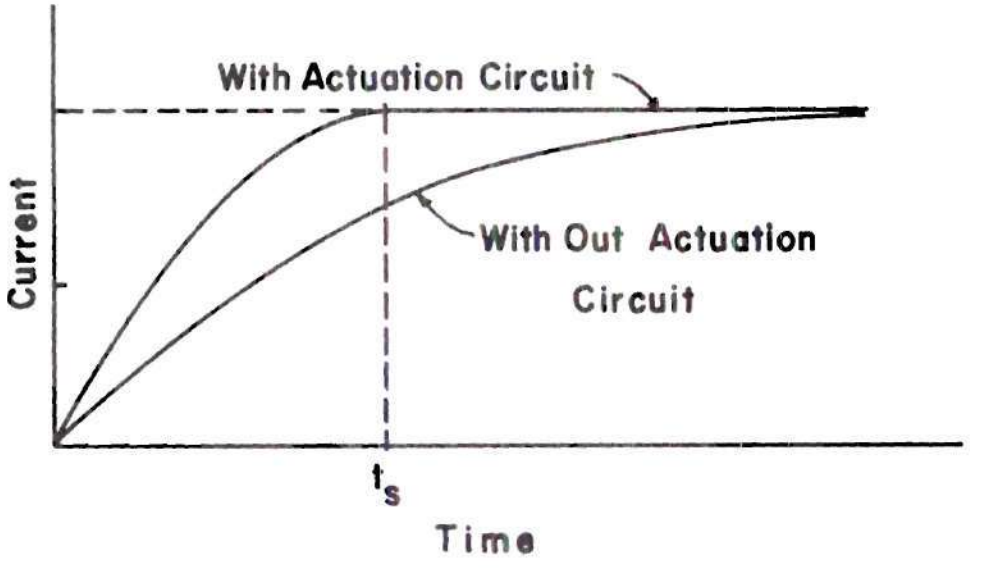

Figure 14. Current Time History of Clutch With and Without Solid-state Activation Circuit

Anderson (28), used several of these circuits in his investigations and found that they reduced the time of response to about one-third its original value on several solenoid-actuated friction clutches.

An additional method of rapid actuation is to power the clutch with a constant current source. Figure 13 shows the constant-current, solid-state device used for clutch actuation in this investigation. The particular choice of circuit design and circuit parameters was to facilitate laboratory use and versatility.

The eighty-volt input was supplied by a standard laboratory vacuum tube power supply. However, it was noted through experimentation that the constant 500 milliampere output current to the fifty ohm load was not affected by the ± 2.5 volt drift in the power supply itself.

Figure 14 shows the current response of a typical clutch when activated with and without the special circuit. This current profile was measured by recording the voltage across a small resistor placed in series with the clutch.

The results of using this circuit will be thoroughly discussed in Chapter III.

Temperature-Dependent Clutch Characteristics

It is widely reported in the literature that electro-

magnetic flux clutches have a built-in torque-limiting characteristic. That is, if the clutch is operated in a constant slip-condition and tends to over-heat, the rise in temperature will increase the coil resistance, hence reducing the current and consequently the torque. A reduction in torque will produce less slip energy to be dissipated. The purpose of the test described here was to determine the effect of temperature on the torque capabilities of a typical magnetic-particle clutch. Both static and dynamic tests were performed.

The static test used the equipment arrangement shown in Figure 10. The special circuit shown in Figure 13 was used to drive a constant current through the clutch. The manual switch allowed the clutch resistance to be monitored during the test. The temperature monitor consists of a strip-chart recorder receiving the amplified output of a thermal couple taped to the clutch body.

The coil was energized and the torque-producing weight was just less than that required to produce slip. The length of time the current flowed was recorded by use of a stop watch.

The dynamic test involved the use of the equipment shown in Figure 11 described above. The input shaft speed

was maintained at one-hundred revolutions per minute. The torque produced by the clutch when activated by the five-hundred milliampere (500 ma) actuation circuit was fifty-seven inch-pounds (57 in.-lbs). As the clutch was operated in total slip, the slip power to be dissipated was approximately sixty-seven watts (67 watts). The coil losses were five watts (5 watts). Therefore, the total power dissipated in the clutch was seventy-two watts (72 watts). The maximum continuous rate of energy dissipation as specified by the manufacturer was seventy-five watts (75 watts).

The results of these tests will be discussed in Chapter III. The data collected is presented in Appendix B.

Two additional points should be noted. No tests were performed on the eddy-current clutch coupling. The reason for this is that its normal size prohibits its use in almost all control applications. Also, since it is a clutch coupling and, hence, must operate in continuous slip, additional problems most certainly would be encountered in any space application.

Also, no endurance tests were performed. The various manufacturers state that electro-magnetic flux devices contain few wearing parts. The manufacturers also attest to reliability investigations involving continuous clutch

cycling at normal rated capacities for over one million cycles.

The tests performed on these clutches are by no means all the possible tests an experimenter might devise. However, it is felt that these give all the data required to forecast the adaptability of the electro-magnetic flux clutch to a space environment.

CHAPTER III

CLUTCH CHARACTERISTICS

This chapter is devoted to a discussion of the collected data on commercially available clutches and to possible applications in a space environment.

Vendor Data Summary

A summary of the data collected from the clutch vendor literature is presented in Table 2. A key to the clutch manufacturers and the clutch models used in the survey can be found in Tables 5 and 6, respectively.

The following is an explanation of the information presented in Table 2. Column one indicates the manufacturer and type of clutch or clutch coupling manufactured. Columns two and three summarize the electrical characteristics of the clutches. That is, the maximum rated d.c. coil current and power dissipated in the coil. It should be noted that the clutch torque is dependent upon coil current and for this reason the manufacturer is able to supply a coil for any d.c. voltage source required by the user. If at all possible, electrical data collected for this survey

were for a 24 vdc source. However, exceptions to this were unavoidable.

Columns four through eight indicate the range of mechanical properties of the clutches manufactured. The maximum transmitted torque is that torque produced by the current listed in column two. This torque level is not the maximum attainable by any particular device but rather is the maximum torque level for continuous non-slip operation. The maximum shaft speed is that for which non-slip operation is possible at the aforementioned torque level. The output rotor inertia is also recorded. Note that in most designs the clutch will accept inputs on either of its shafts. However, from an efficiency aspect it is beneficial to use the rotor with least inertia as the output. The time response is that time required for the clutch torque level to attain 63 per cent of its steady-state level when actuated by a step voltage. The maximum transmitted power is the product of maximum torque and maximum shaft speed.

Columns nine and ten indicate the physical data of the clutches manufactured. Namely, total volume or displacement and total weight. In many cases the clutch is mounted directly on shafts and gears with a slip-ring electrical connection. However, the stationary body clutches require a

designed mounting. In these cases the factory-equipped mounting was included in the volume and weight data. Also, over-all length exclusive of shafts and the largest clutch dimension exclusive of slip-rings were used in the volume calculations.

Columns eleven through fourteen list the various performance indices used in rating clutches. These values were calculated using the aforementioned data. The power ratio or power gain listed in column 14 is obtained by dividing the coil power into the maximum transmitted power value. This does not imply that the clutch acts as a linear power gain but is intended to give an estimate of the maximum possible power gain attainable.

Most of the manufacturers listed several clutch models. Each model exhibited different characteristics. In these cases, the range of values of each column is indicated for each manufacturer by rows labeled "minimum" and "maximum." Therefore, for manufacturer "A" the clutch requiring 104 milliamperes excitation is not necessarily the same clutch with maximum torque of 0.375 inch-pounds.

Anderson (29) presents some characteristic data for mechanical contact clutches. In almost every case these clutches show greater torque to weight and torque to volume

Table 2. Clutch Vendor Data Survey

Clutch Type	1 Manufacturer Code	2 Maximum Coil Control Current (mamp)	3 Maximum Control Power (watts)
Hysteresis	A		
	Minimum	104	2.50
	Maximum	292	12.00
Hysteresis	B		
	Minimum	125	3.00
	Maximum	417	10.00
Hysteresis	C		
	Minimum	30	0.11
	Maximum	300	7.20
Hysteresis	D		
	Minimum	71	0.17
	Maximum	332	7.96
Magnetic Particle	E		
	Minimum	23	2.10
	Maximum	920	45.90
Magnetic Particle	F	165	3.96
Magnetic Particle	G	165	3.96
Magnetic Particle	H		
	Minimum	35.6	0.855
	Maximum	558	13.400
Magnetic Particle	I		
	Minimum	8	0.53
	Maximum	575	11.60

Table 2. (continued)

4 Maximum Transmitted Torque (in.-lb)	5 Maximum Shaft Speed (rpm)	6 Output Rotor Inertia J x 10^4 (in.-lb-sec^2)	7 Time Response (63% of Max Torque) (msec)
0.375	4,000	0.186	28
21.875		24.000	45
0.313	5,000	0.180	N/A
22.500	18,000	24.000	
0.156	15,000	N/A	N/A
21.875	30,000		
0.125	3,600	0.040	N/A
25.000		53.000	
1.313	3,600	0.024	40
200.	12,000	5.050	1160
4.688	3,500	0.019	2.3
4.688	3,500	N/A	4.0
0.188	3,500	0.0005	0.17
17.500		0.1844	2.47
0.313	1,000	0.028	7.5
1900.	3,400	1000.	250.

Table 2. (continued)

8	9	10	11
Maximum Transmitted Power (watts)	Gross Clutch Displacement ($in.^3$)	Gross Clutch Weight (lb)	Torque / Weight (in-lb/lb)
16.55	0.184	0.419	0.895
1035.	68.000	12.500	2.980
74.30	3.65	0.500	0.626
1330.	170.	34.500	2.000
55.50	0.855	0.169	0.924
3880.	86.800	12.500	1.751
5.33	N/A	0.313	0.399
1065.	83.10	12.500	2.000
186.5	13.82	2.000	0.526
8520.	2720.	233.	0.859
194.	3.05	0.563	8.310
194.	3.05	0.500	9.376
7.79	0.381	0.063	2.990
725.	14.24	3.000	8.750
3.70	0.248	0.055	5.000
22,500.	470.	80.000	23.750

Table 2. (continued)

12 Torque Volume (in.-lb/in.^{3})	13 $\frac{\text{Torque}}{\text{Inertia}} \times 10^{-4}$ (in.-lb/in.-lb-sec^2)	14 Power Out Power In (watt/watt)
0.297	0.281	6.62
2.040	2.015	346.
0.133	0.608	24.75
1.065	3.455	133.00
0.140	N/A	18.50
0.265		712.
0.143	0.353	6.580
0.306	4.700	185.
0.046	0.260	29.30
0.095	1242.	128.70
1.535	240	49.0
1.535	N/A	49.0
0.494	94.7	9.12
2.020	622.	54.20
1.262	0.222	28.11
4.670	25.000	1940.

ratios than the magnetic flux devices. Also, for comparable torque levels, certain of the friction devices (e.g., wrap spring clutch) exhibit a greater power gain than their magnetic flux counterparts.

However, the magnetic flux devices have two distinct advantages over the mechanical contact device. First, the magnetic-particle clutch may be operated in continuous slip and is bi-directional with relation to shaft rotation and energy flow. This is not necessarily true with mechanical contact clutches.

Experimental Results

The results of the experimental procedures discussed in Chapter II are presented in this section.

The first test performed was to ascertain the relation between the coil current and the resultant output torque in a static condition. This test involved the equipment arrangement shown in Figure 10.

As the tests were performed it was apparent that the magnetic-particle clutch exhibited a property not present in the hysteresis device. That is, unless the particles within the working gap of the clutch were well distributed, the clutch underwent a condition of slip when loaded to a level less than its rated slip-torque for any given current

level.

If the magnetic-particle clutch shown in Figure 7 is not rotating and is de-energized its particles will tend to follow the action of any gravitational field present. The particles will then be gathered in only a portion of the working gap. Hence, upon energizing the coil the clutch torque capabilities will be impaired until an even distribution is again achieved in the working gap. The equipment arrangement used in the laboratory allowed this phenomenon to be more easily investigated.

Figure 15 shows a typical torque history during one test at a single current level for a magnetic-particle clutch. The clutch was energized by a constant current and loaded with a static torque by means of the water weight.

Point (A) on curve I is the point of initial slip. Here, because of the uneven distribution of particles in the working gap, the clutch slipped at a torque level of 50 per cent to 70 per cent of its normal capacity for that current. At this point of initial slip the relative rotation between input and output was 30 to 60 degrees.

During the initial slip, the particles were physically redistributed in a more uniform manner. This allowed the loading to continue to an higher torque level without

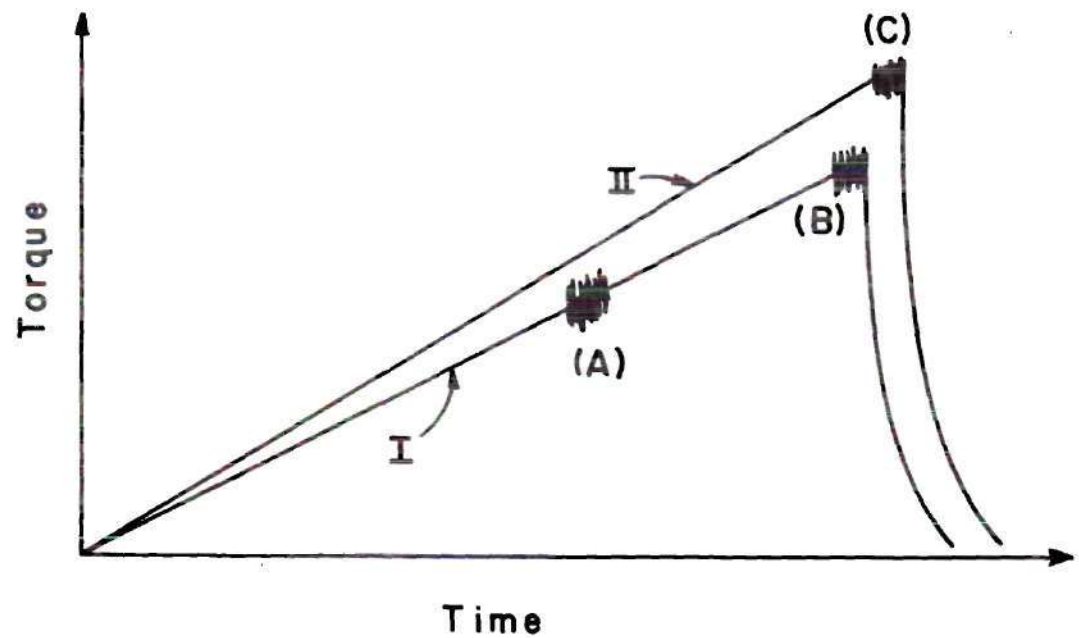

Figure 15. Typical Static Torque Test Result
(Magnetic Particle Clutch)

increasing the current. Finally, however, a point was reached at which time the clutch slipped more than three full revolutions. This corresponding torque level is denoted in Figure 15, curve I as point (B) and has been nomenclated as the point of final slip.

The clutch was not de-energized (at this time), but rather was forced to slip through five additional rotations. Then it was reloaded using the water weight and resulted in curve II, Figure 15. The point (C) is, again, the torque level at which the clutch experienced total slip.

The data recorded in these tests were torque values at which initial, total and distributed particle slippage took place for each value of current energizing the clutch. Specifically then, points (A), (B), and (C) were plotted for various values of current (I) for each clutch. A typical result is shown in Figure 16.

Appendix B contains a detailed presentation of the test data collected in the laboratory. The static torque test results for the laboratory-tested clutches can be found in Figures 33, 43, 49 and 55.

The hysteresis clutch did not exhibit a condition of partial slippage as noted in the magnetic-particle clutch. The static torque-current relationship for the hysteresis

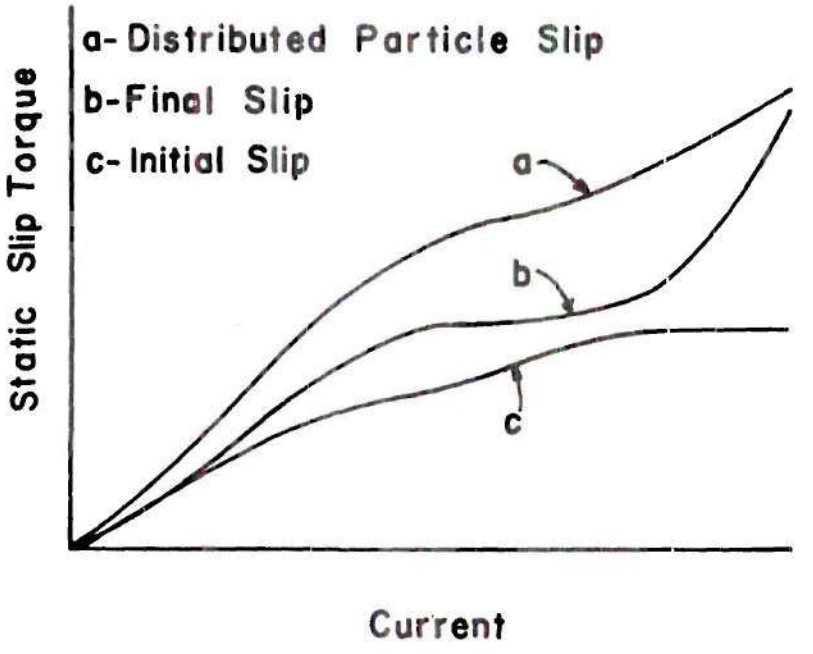

Figure 16. Static Slip Torque vs. Current for Clutch I-5

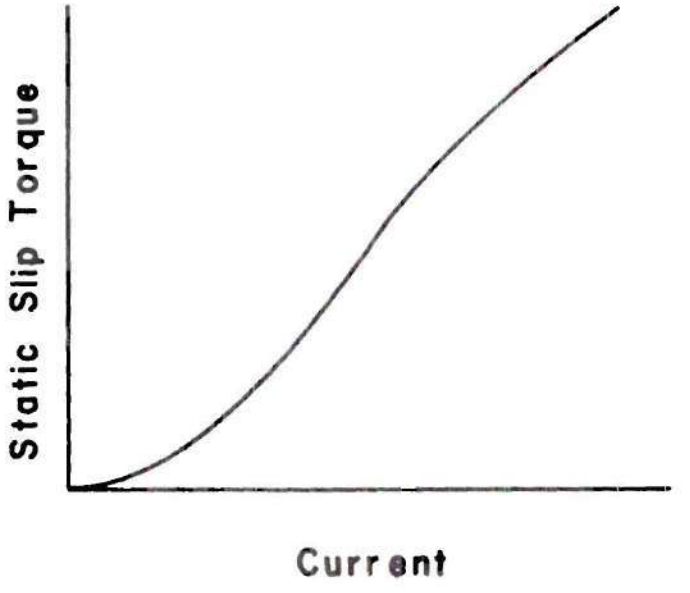

Figure 17. Static Slip Torque vs. Current for Clutch D-4

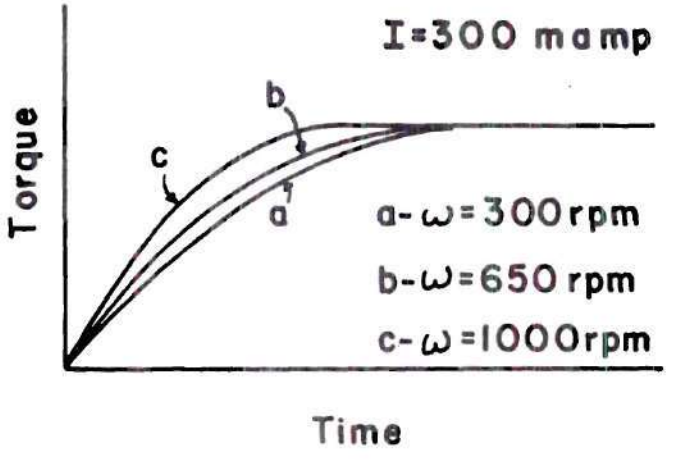

Figure 18. Torque Build-up at Various Slip-Speeds for Clutch I-5

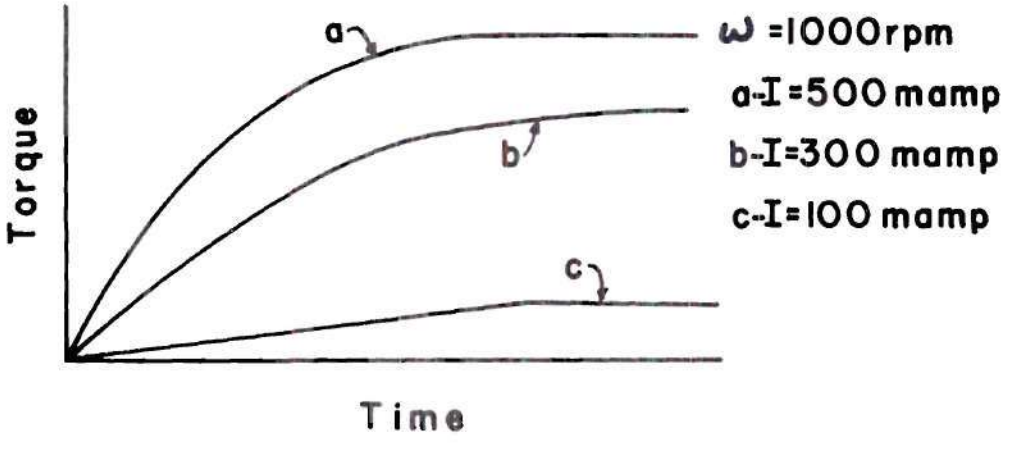

Figure 19. Torque Build-up as a Function of Steady-State Current Level for Clutch I-5

clutch is given in Figure 17.

The remaining tests performed in the laboratory pertained to the recording of the torque time history for various conditions of operation. The test procedure is described in Chapter II. The equipment arrangement is shown in block diagram form in Figure 11.

It was experimentally determined that the time required for the magnetic-particle clutch to achieve its maximum torque carrying capability is dependent upon both the slip-speed during activation and the magnitude of the clutch coil current.

Figure 18 shows a typical time history of torque build-up during actuation for various values of slip-speed. It should be remembered that the slip-speed noted in each case was constant throughout the activation. This would not be the case if the output shaft were accelerating to the speed of the input shaft.

The reason for the reduction in response time is attributed to the time required for distribution of the particles in the working gap of the clutch itself. This distribution is accomplished almost exclusively by the relative motion between the clutch body and the torque-carrying umbrella attached to the output shaft. However, the response

time was not reduced when the slip-speed was made greater than 1000 revolutions per minute. Figures 34, 44, 50 and 56 in Appendix B show additional examples of this test result.

All tests performed in the laboratory involved activation of the test clutch by one of two means. For rapid activation of the clutch the special circuit shown in Figure 13 was employed. However, for normal conditions and unless otherwise stated, the circuit shown in Figure 12(a) was employed. Therefore, under normal conditions the current build-up in the clutch follows the relationship given in equation (2.1). As a result of the linearity of the circuit, the time required to build-up current to the steady-state value of equation (2.1) is independent of the magnitude of the steady-state current level. Since the torque-carrying capability of the clutch is directly proportional to the coil current it might be thought that the torque time response is also independent of the steady-state current level. That this is not the case is shown in the following test.

The test clutch was actuated by at least three different current levels. Figure 19 shows a typical test result. Similar results for the other clutches tested may be

found in Appendix B.

The reason for the variation in response time may again be attributed to the time required to distribute the magnetic particles evenly about the working gap. It has been previously stated that the particles are distributed by the action of the relative motion of output umbrella and clutch body. The result of this test indicates that the particles are also influenced in their migration by the magnetic flux force.

Similar results to the above discussion were found for the case of torque decay. This data is presented also in Appendix B. Also, it is noted that the hysteresis clutch (D-4) did not exhibit the aforementioned properties. Again, this results from the fact that there is no working medium.

The hysteresis device did demonstrate a slower reaction to the torque-inducing current. This is a result of its basic means of operation as explained in Chapter I.

Actuation tests were performed on each clutch using the specially designed quick-actuation circuit. The effective steady-state current range of the circuit was 400 to 500 milliamperes. The current build-up and decay for these extremes are shown in Figures 20 and 21, respectively. This current profile was not affected by the individual clutch

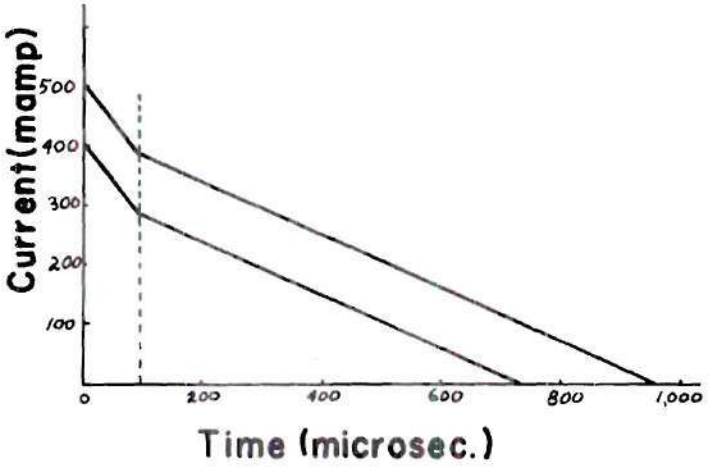

Figure 20. Current Decay with Quick Activation Circuit

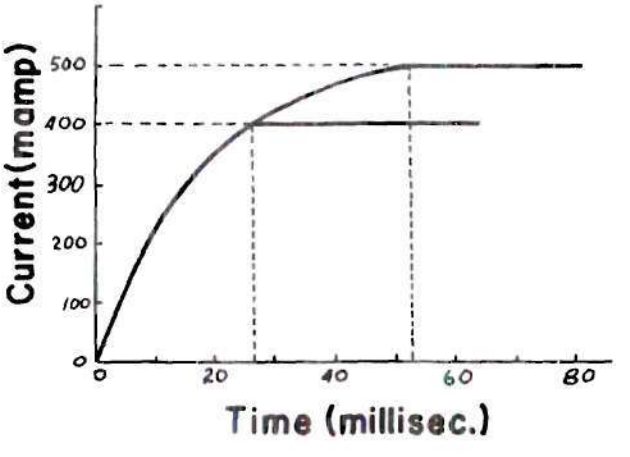

Figure 21. Current Build-up with Quick Activation Circuit

connected to the output of the circuit.

The results of the quick actuation tests are presented in Figures 40, 41, 46 and 47 of Appendix B. The special actuation circuit did improve the time response of the torque build-up. However, the torque decay time was not appreciably improved.

Electromagnetic flux clutch devices display operating characteristics similar to those of the mechanical contact clutches investigated by Anderson (1). That is, both types of devices have a somewhat linear relationship between the output torque and control variables. The fluid couplings described by Jones (2) do not have this linear operational characteristic.

In general, the electromagnetic flux device is not as fast-acting as the friction device, taking as much as three times as long to complete the same operation. However, certain specially designed magnetic-particle clutches having low torque-carrying capabilities are capable of attaining 63 per cent of their steady-state torque level in two or three milliseconds.

The smoothness of engagement allows the electromagnetic flux device to perform in applications not capable of accepting impact loading. Also, electromagnetic flux

clutches and clutch couplings are capable of indefinite periods of asynchronous operation without failure, wear or adjustment.

Clutch Input Power Requirements

All electromagnetic flux clutches require an electrical current for activation and sustained operation. The form and magnitude of the current is almost completely adaptable to the design application. Most commonly, the clutch requires a d.c. current but various manufacturers will supply a.c. units.

Additional types of magnetic flux coupling and clutch couplings do operate by use of permanent magnets and electrostatically-charged particles. However, these units are specially designed and do not appear to be commercially available.

Table 2 gives an indication of the range of input power requirements of magnetic-particle and hysteresis clutches used in this country. In addition, an eddy-current clutch coupling rated for 3/4 horsepower at 1800 rpm or 1½ horsepower at 3600 rpm typically requires excitation of one ampere at 40 volts or 0.380 amperes at 90 volts.

Types of Clutch Failure

No endurance tests were performed on the clutches investigated in the laboratory, because information supplied in the vendor literature stated that typical electro-magnetic flux devices are capable of several million duty cycles without failure, repair or adjustment. These statements, by manufacturers, are collaborated in the current technical literature.

Electromagnetic flux clutches are subject to various types of failure, however. These include bearing failure as a result of contamination or lack of lubrication, electrical brush failure in the case of rotary body clutches, electrical insulation break-down resulting from insufficient heat transfer; and in the case of magnetic-particle clutches, contamination of the particle dust in the working gap.

In comparison, those mechanical contact clutches capable of slip operation produce wear products, may require periodical adjustment and are capable of complete failure when subjected to continuous over-load. Those mechanical contact clutches not capable of slip operation will fail as a result of over-load.

Also, hydraulic clutch-couplings are subject to changes in fluid viscosity and density which may impair or prevent their normal operation.

Temperature Dependent Characteristics

Test clutch I-5 was subjected to the tests described in Chapter II to determine its operating characteristics when subjected to a rising temperature.

The static test was primarily to determine the amount of electrical resistance increase as a result of constant current coil excitation. The coil excitation was maintained at 500 milliamperes for a period of 45 minutes by use of the special quick actuation circuit of Figure 13. The clutch coil electrical resistance increased approximately one ohm as the clutch temperature rose approximately ten degrees Fahrenheit.

However, as this was a static test it was noted that oxidation and possible arcing of the slip-rings caused the total clutch circuit resistance to rise approximately seven ohms. It is therefore concluded that no appreciable increase in coil resistance can result from electrical power losses.

The dynamic test required 22 minutes to complete. The coil current was maintained at 500 milliamperes and the slip-torque of the clutch was also maintained constant at a level of 57 inch-pounds. The coil resistance was initially 19.8 ohms at an ambient temperature of 184.0 degrees

Fahrenheit. The test clutch attained a temperature of 184.0 degrees Fahrenheit when the test was stopped. The coil resistance was measured at 25.3 ohms. If the clutch had been activated by normal activation circuit using a constant voltage power supply this increase in coil resistance would have reduced the torque capability of the clutch from 57 inch-pounds to 54 inch-pounds.*

The results of this test indicate that as the coil resistance rose 29 per cent over its original value the torque was reduced by 5 per cent and the power dissipation was reduced by 10 per cent. This does not appear to be as significant a reduction in slip energy as required to save the clutch from over-heating and sustaining permanent damage.

In conclusion, it would appear the designer must make allowance for changes in coil resistance as a result of temperature change if close torque control is required. One method of accomplishing this end is a compensating resistor available for individual clutches from the manufacturers.

*This was established in the laboratory by reducing coil current until the coil voltage was the same as at the start of the test.

CHAPTER IV

ANALYTICAL RELATIONSHIPS OF ELECTRO-MAGNETIC FLUX CLUTCHES

From a historical standpoint, the electro-magnetic flux clutch has not found application in design situations requiring precise mathematical representation. Consequently, in general, mathematical models for the various flux clutches are not available. The single exception is the magnetic-particle clutch for which a frequency analysis has been performed by Blackburn (30).

The present chapter will summarize the analytical and empirical mathematical models available from the literature. Whenever possible, correlation will be drawn with the author's own experimental results as presented in Chapter III.

Steady-State Torque Current Relationship

It has been previously stated that the steady-state or maximum torque capability of any electro-magnetic flux clutch is dependent upon the coil current excitation. Also, the force of attraction between separated magnetic poles is a function of the square of the flux density in the working

gap of the clutch. Since the flux density is a linear function of the current it can be inferred that torque is related to current according to the equation

$$T = bI^2 \qquad (4.1)$$

where b is a constant characteristic of the clutch. Parziale and Tilton (19) found that in the case of a fluid-magnetic-particle clutch equation (4.1) is not precisely true. They suggest the more general form

$$T = bI^n, \qquad 1 \leq n \leq 2 \qquad (4.2)$$

with b and n characteristic of the individual clutch.

Blackburn (30) has found that equation (4.1) does adequately describe the dry-particle clutch presently available from industrial sources.* However, it should be pointed out that a certain amount of confusion may exist from an improper interpretation of this equation.

Throughout the literature equations (4.1) and (4.2) are referred to as the "static torque-current" relationship. This nomenclature does not imply any rotationally static situation. Rather, it describes the situation of impending slip between input and output shafts when the clutch is

*The constant "b" in equation (4.1) is extremely sensitive to changes in clutch temperature.

transmitting maximum torque at its rated rotational velocity. Hence, static in this sense implies zero slip velocity at maximum torque.

For the purpose of this discussion equation (4.1) is referred to as the steady-state torque current relation. This change in nomenclature is a result of the data already presented in Chapter III, Figure 16, as static torque-current data. It is evident that the data of Figure 16 does not fit either equation (4.1) or (4.2).

Figure 17 presents the steady-state torque-current data collected in the laboratory for the hysteresis clutch (D-4). This data represents both the static and steady-state relationships since the hysteresis clutch has no working medium. A least-square fit was applied to this data using the functional form of equation (4.2). The result is

$$T = 45.0(I)^{1.85} \qquad (4.3)$$

No eddy-current clutch was tested in the laboratory. For this reason no similar data can be offered for comparison. However, from the literature, Swords (25), a typical torque-current-slip speed relation is presented in Figure 22.

Frequency Response

Blackburn (8) has developed a lumped parameter transfer function for the dry magnetic-particle clutch from frequency response data. A summary of this work is presented in the current literature by Grau and Chubb (22). In addition, Blackburn demonstrates a technique for manipulating the transfer function in the analysis of a clutch servo system. Only the mathematical relationships found in this work will be presented. Further information may be found in the original work or in the alternate reference by Grau and Chubb.

For a dry magnetic-particle clutch with a non-laminated core as shown in Figure 7, the transmitted torque is given by,

$$T = 5.59 \times 10^{8} \ (f \ K_q \ R/A) \ \varphi^2 \qquad (4.4)$$

where

T = transmitted torque, (in.-lb)
f = coefficient of kinetic friction for dry powder
A = cross-sectional area of powder gap normal to flux ($in.^2$)
K_q = $\frac{\text{actual area occupied by particles}}{\text{available area normal to flux lines}}$
φ = total flux through working gap (webers)
R = radius to clutch shear surface (in.)

In the case of the steady-state transmitted torque previously discussed in this chapter, the flux can be linearly related to the current level in the clutch by the relationship

$$\varphi = NI/(R_g + \sum_i R_i) \qquad (4.5)$$

where

N = number of turns in coil (turns)
I = current (amperes)
R_g = effective reluctance of gap and powder (1/henry)
R_i = sum of reluctance about path exclusive of gap (1/henry)

The transfer function which relates the flux to the current in the coil is rather complex. This is a result of hysteresis and eddy-current coupling effects and losses. The expression found by Blackburn is

$$\frac{\varphi(s)}{I(s)} = \frac{K(\tau_1 s + 1)}{(\tau_2 s + 1)} \left(\frac{\varphi(0)}{U(0)}\right) \left(\frac{\tanh \sqrt{as}}{\sqrt{bs}}\right) \qquad (4.6)$$

where

$\varphi(s)$ = total flux
$I(s)$ = signal current
τ_1, τ_2 = time constants
K = linear gain
$\frac{\varphi(0)}{U(0)}$ = static gain of total flux vs. flux density at gap boundary
a, b = characteristic constants

The evaluation of the constants of (4.6) can be accomplished by physical measurement of the clutch parameters. Each of the constants in (4.6) can be related to a physical quantity as shown in Grau and Chubb.

Result (4.4) relates torque and flux in the time domain. Result (4.6) relates flux and current in the frequency

domain. The proper inversion of equation (4.6) allows one to relate torque and current in the time domain by use of equation (4.4).

No similar analysis has been performed on either the hysteresis clutch or the eddy-current clutch coupling. This is a definite area for further work if full use is to be made of the capabilities of these devices.

Hysteresis and Eddy-current Effects

Every electro-magnetic flux device experiences both eddy-current and hysteresis losses. The magnitude of these effects on the torque characteristics of the clutch is totally dependent upon the particular clutch design. For example, eddy-current losses can be reduced by constructing the core of some laminated material.

Winston (4) has developed a set of semi-empirical relationships which allow one to calculate the magnitude of both the hysteresis and eddy-current coupling in a hysteresis clutch.

Before the hysteresis clutch begins to slip, its torque capabilities are

$$T_h = 11.3\ P\ V\ W_h \qquad (4.7)$$

$$= 111\ H_{2max}\ P\ R \times 10^{-5} \qquad (4.8)$$

where

$$H_{2max} = \frac{W_h \times 10^5}{B_{rmax}} \qquad (4.9)$$

and,

T_h = hysteresis torque (in.-oz)
P = number of poles
V = volume of hysteresis ring (in.^{3})
W_h = hysteresis loss in ring (joules/in.^{3}/cycle)
H_{2max} = coercive force corresponding to the maximum flux density in the ring (amp-turns/in.)
φ = flux per pole (kilolines)
R = mean radius of ring (in.)
B_{rmax} = maximum flux density in ring (kilolines/in.^{2})

It has previously been stated that eddy-current coupling cannot take place unless there is some relative motion between input and output rotors. When such slippage does take place the hysteresis torque given by equations (4.7) or (4.8) are still valid. The additive eddy-current torque is then given by

$$T_e = \frac{0.25 \times 10^{-15} P B_{avg}^2 L_c R^2 \lambda t (\omega_1 - \omega_2)}{\rho} \qquad (4.10)$$

where

T_e = eddy-current torque (in.-oz)
B_{avg} = average flux density over a pole pitch (lines/in.^{2})
L_c = axial length of hysteresis ring (in.)
λ = pole pitch (in.)
t = radial thickness of ring (in.)
ρ = resistivity of ring material (ohms/in.^{3})
ω_1 = input rotor speed (rpm)
ω_2 = output rotor speed (rpm)

Although relationships (4.7) through (4.10) were

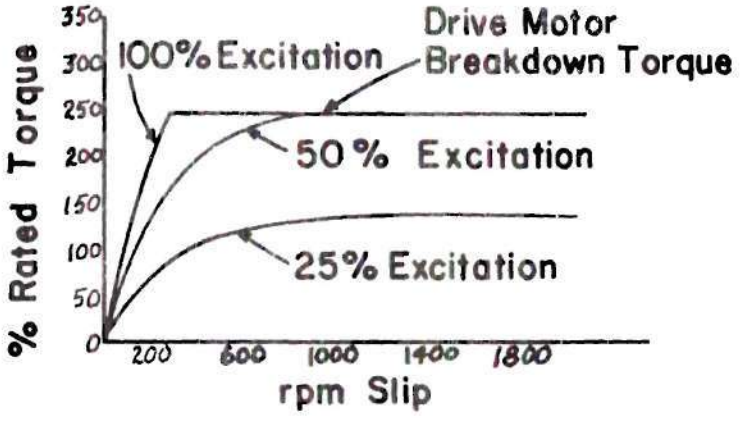

Figure 22. Operating Characteristics of a Typical Eddy-current Clutch Coupling

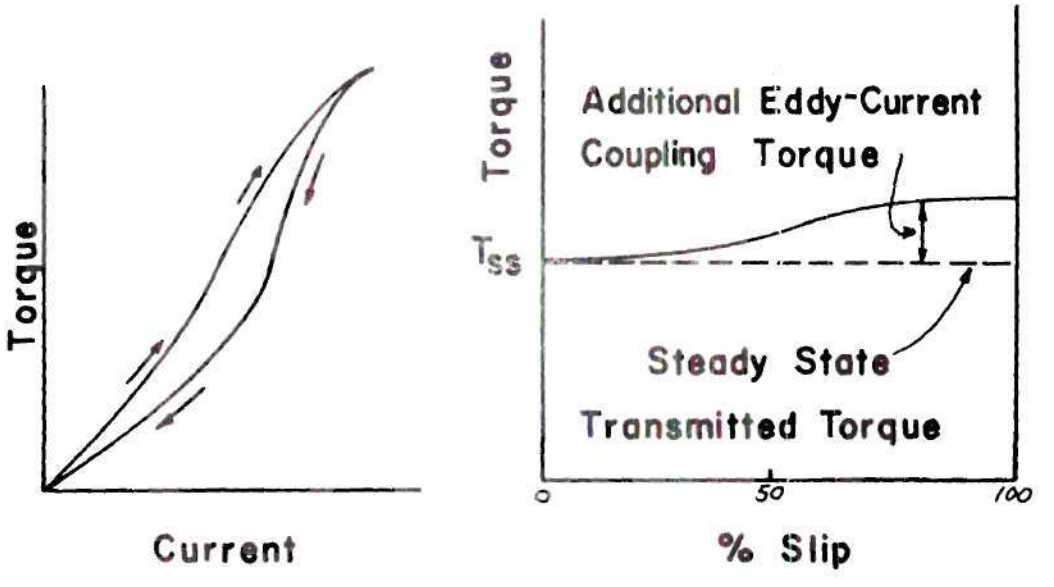

a) Hysteresis b) Eddy-current

Figure 23. Hysteresis and Eddy-current Effects upon Steady-State Torque Levels

specifically developed for a hysteresis clutch, the proper evaluation of the various terms should allow their application to any electro-magnetic flux device. The effect which hysteresis might have on a typical electro-magnetic flux device is shown in Figure 23(a). Here it can be seen that hysteresis acts as an additional non-linear component. The effect of eddy-current coupling is shown in Figure 23 (b). Note that in this case, increases in slip-speed tend to increase the torque carrying capabilities of the device.

Glasenko (31) and Vorob'yeva (6) consider the more involved calculations of clutch design. The former is solely concerned with asynchronous or hysteresis type clutches and develops an optimal expression for the number of pole-pairs in any particular configuration. The later considers all possible types of electro-magnetic flux clutches and serves as a good summary of clutch design techniques.

In related areas, Flidlider (23) and Vorob'yeva (6) both analyze the transient response of magnetically actuated friction disc clutches. Also, Young (37) discusses the use of permanent magnet couplings and develops several analytical expressions.

CHAPTER V

CLUTCH ENERGY DISSIPATION

All previous discussions of clutch performance have been based upon the mechanical or electrical properties of the clutch. However, the thermal properties of the clutch may also seriously affect clutch operation.

If the clutch is required to perform some cyclic or over-load operation it is evident that energy will be dissipated in the clutch whenever it is in a slip condition. This energy will be dissipated through some form or combinations of forms of heat transfer. In addition, the body temperature of the clutch will rise. This increase in clutch temperature may cause clutch failure as a result of a break-down in electrical insulation within the clutch itself.

Table 3 gives a summary of the AIEE Standard, No. 1, general classification of electrical insulating materials. The majority of commercially available clutches are constructed with Class A insulation and the remaining few with Class B. Preliminary inquiries indicate that manufacturers could use higher temperature insulators if the increase in

Table 3. Classification of Electrical Insulators

Class		Description	Temperature Limit
O		Cotton, silk, paper and similar organic materials when neither impregnated nor immersed in a liquid dielectric	90° C
A	1.	Cotton, silk, paper and similar organic materials when either impregnated or immersed in a liquid dielectric;	
	2.	Molded and laminated materials with cellulose filter, phenolic resins and other resins of similar properties;	
	3.	Films and sheets of cellulose acetate and cellulose derivatives of similar properties;	
	4.	Organic varnishes or enamels when applied to conductors	105° C
B		Mica, glass fibre, asbestos, etc., with suitable bonding substances. Other materials which show capabilities to operate at Class B temperature	130° C
H		Materials or combinations of materials such as silicon elastomer, mica glass fibre, asbestos, etc., and other suitable materials for Class H temperatures	180° C
C		Mica, porcelain, glass quartz and similar inorganic materials	As specified in excess of 180° C

performance justifies the necessary increases in weight and/or bulk.

Slip energy may be removed from the clutch in any one or combination of the means of heat transfer; namely, convection, conduction, and thermal radiation. A cursory discussion of convection and conduction will be given with references. A more complete discussion of thermal radiation will be presented. In addition, a general mathematical expression will be given for the slip energy developed in the clutch during a cyclic operation and a design procedure will be indicated such that the slip energy may be minimized.

Conductive and Convective Heat Transfer

Anderson (1) gives a complete analysis of clutch energy dissipation by conduction. He assumes that the clutch is solidly mounted on some n-member compound structure each component of which has a thermal resistance R_i. Then, if the clutch temperature is T_c and the base temperature T_b, the general conductive heat transfer Q_c is given by

$$Q_c = \frac{T_c - T_b}{\sum_{i=1}^{n} R_i} \tag{5.1}$$

Expression (5.1) is capable of producing a serious error in calculation if information on the contact conductance

of the various clutch mounting components is not known. Anderson gives references and data on the variations in contact conductance and shows a numerical example assuming the clutch to be constructed of aluminum and the base of molybdenum.

Slocum (32) considers the convective qualities of the magnetic-particle clutch. In reality, when a rotary body clutch is operated in an atmosphere, the clutch body rotates and hence there is a certain amount of forced convection as the clutch rotates in the stationary atmosphere. If the amount of energy developed in the clutch from slippage is denoted by q_{in}, then the temperature of the clutch, T_c, is found to be

$$T_c = \frac{q_{in}}{hA} \left(1 - \text{Exp}\left(- \frac{(hA)t}{wC_p}\right)\right) + T_a \qquad (5.2)$$

where

q_{in} = mechanical input power (BTU/hr)
t = temperature (^{o}F)
C_p = heat capacitance (BTU/lb-^{o}F)
h = convective heat transfer coefficient (BTU/hr-ft^2-^{o}F)
A = surface area (ft^2)
w = weight density (lb/ft^3)
T_c = clutch temperature (^{o}F)
T_a = ambient temperature (^{o}F)

In practice, however, values of h, the convective heat transfer coefficient, are only tabulated for objects

placed in cross-flow. Slocum proposes that the introduction of two empirical correction factors into result (5.2) will account for the error in evaluating the h quantity and the difference in configuration between a cylinder in cross-flow and a rotating clutch. This modified expression for the clutch temperature is

$$T_c = \frac{q_{in}}{\alpha_T hA} \left(1 - \text{Exp}\left(- \left(\frac{\alpha_t hA}{C_p}\right) t\right)\right) + T_a \qquad (5.3)$$

Slocum presents a detailed method for evaluating the correction factors α_T and α_t. These factors are used in equation (5.3) with the appropriate data to generate so-called heating and cooling curves to be used in a clutch design procedure.

It is worth noting that in most space applications there will not be an atmosphere present for convective heat transfer. The purpose then in presenting this material is to indicate a workable method from which extensions may be made to other forms of heat transfer.

Certain clutch designs will allow the introduction of a coolant to the area of slip-energy generation. This is the case for clutches manufactured by manufacturer E. This design may be adapted to the other types of clutches

commercially available but only with an increase in weight and bulk. Also, some type of coolant reservoir and heat exchanger are necessary.

Radiant Heat Transfer

In any space application there are two primary means of heat transfer available in the absence of an atmosphere. These are conduction and radiation. If the clutch in question is a rotary body type, it is connected to its surroundings only by gears and/or shafts. This necessarily reduces its means of conducting away energy and increases the importance of thermal radiation.*

As with all mathematical analyses of real systems, certain assumptions must be made in order to allow the analysis. The first of these assumptions is that the clutch has attained a steady-state temperature. Since the temperature of the clutch remains constant, the energy being generated within the clutch per unit time and the energy radiated to the surroundings per unit time must be equal. That is,

$$Q_{in} = Q_{out} \tag{5.4}$$

Also, it is assumed that the clutch is completely

*Radiation is considered to be the major means of energy transfer.

enclosed by its surroundings. In order to simplify the analysis, let the clutch and its surroundings appear as concentric spheres or co-linear cylinders, each exhibiting gray-body characteristics.

Krieth (33) shows that the energy transfer for the case described above can be represented in terms of an electrical circuit. Figure 24 shows this equivalent circuit.

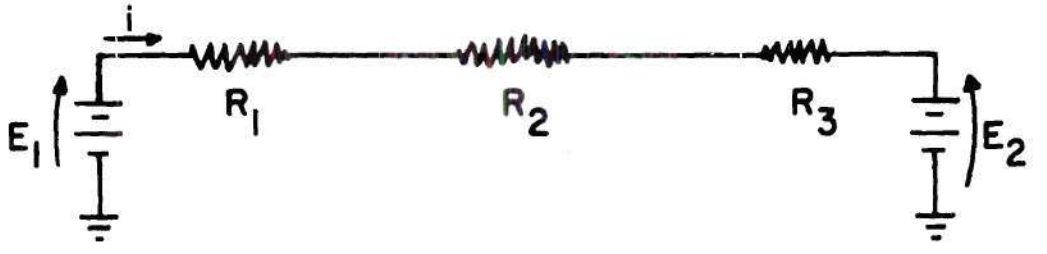

Figure 24. Electrical Equivalent for Gray-body Radiation for Concentric Spheres

The net current flow for the circuit of Figure 24 is

$$i = \frac{E_1 - E_2}{R_1 + R_2 + R_3} \qquad (5.5)$$

The algebraic terms of equation (5.5) have the following equivalence with the physical and thermal quantities of the system:

$$i = Q \qquad (5.6)$$

$$E_1 = \sigma \bar{T}_1^4 \tag{5.7}$$

$$E_2 = \sigma \bar{T}_2^4 \tag{5.8}$$

$$R_1 = \rho_1 / A_1 E_1 \tag{5.9}$$

$$R_2 = 1/A_1 F_{1-2} = 1/A_2 F_{2-1} \tag{5.10}$$

$$R_3 = \rho_2 / A_2 \quad 2 \tag{5.11}$$

Making the substitutions indicated by relationships (5.6) through (5.11), equation (5.5) becomes

$$Q = \frac{\sigma (\bar{T}_1^4 - \bar{T}_2^4)}{\frac{\rho_1}{A_1 \ 1} + \frac{1}{A_1 F_{1-2}} + \frac{\rho_2}{A_2 \ 2}} \tag{5.12}$$

From the gray-body assumption,

$$\epsilon_1 + \rho_1 = 1 \tag{5.13}$$

and since the surroundings and clutch are assumed concentric spheres, the shape factor, F_{1-2}, is identically unity. With these modifications, expression (5.12) becomes

$$q = \frac{Q}{A_1} = \frac{(\bar{T}_1^4 - \bar{T}_2^4)}{\frac{1}{\epsilon_1} + \frac{A_1}{A_2} (\frac{1}{\epsilon_2} - 1)} \tag{5.14}$$

The maximum amount of energy transfer will take place when the clutch body has achieved its maximum safe operating temperature. For a clutch constructed with Class A electrical insulation this temperature is 105° Centigrade or 681°

Rankine. The surroundings may be assumed to be at a standard temperature of 70^{o} Fahrenheit of 530^{o} Rankine.

As a further simplification, it will be assumed that the emissivity of both the clutch and its surroundings are the same. Hence,

$$\epsilon_1 = \epsilon_2 = \epsilon \tag{5.15}$$

Applying (5.15) to (5.14) results in the following final form for the radiant heat transfer from the clutch to its surroundings:

$$q = \frac{Q}{A_1} = \frac{\epsilon\sigma(\bar{T}_1^4 - \bar{T}_2^4)}{1 + (1 - \epsilon)\frac{A_1}{A_2}} \quad . \tag{5.16}$$

Figure 25 shows the result of evaluating equation (5.16) for values of ϵ and area ratio A_1/A_2. The range of emissivity was chosen to include most all metals or metallic surfaces. It is naturally advantageous to have the clutch and surroundings made of a material with an high emissivity. The area ratio of 0.00 indicates the limiting case of the clutch appearing to be a point in space compared with the surroundings. An area ratio of 1.00 is representative of the opposite extreme when the surroundings are so near the clutch that both appear to have equal lateral area.

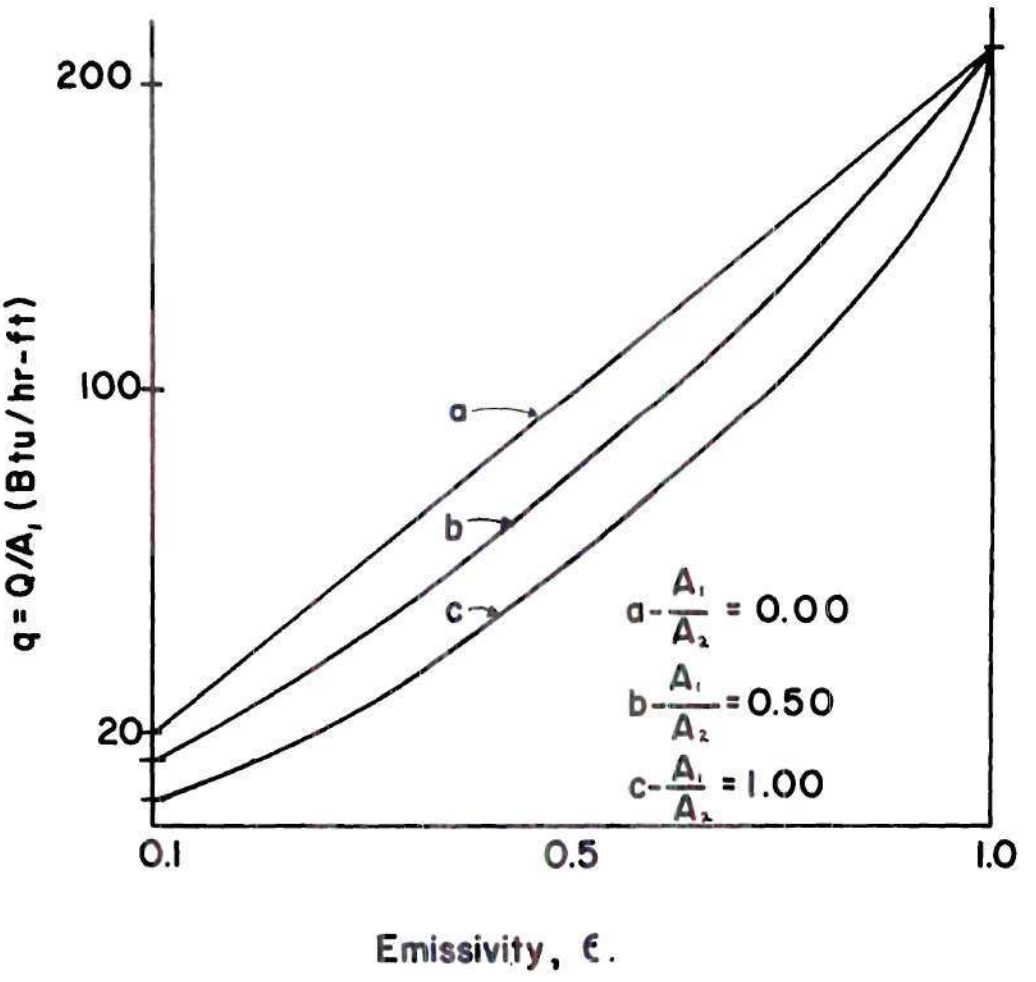

Figure 25. Radiant Clutch Energy Dissipation as a Function of Emissivity and Area Ratio

Table 4. Radiant Clutch Energy Dissipation, $\frac{BTU}{hr\text{-}ft^2}$

ϵ \ $\frac{A_1}{A_2}$	0.00	0.10	0.20	0.30	0.40	0.50	0.60	0.70	0.80	0.90	1.00
0.10	20.79	19.07	17.62	16.37	15.29	14.34	13.50	12.75	12.09	11.48	10.94
0.20	41.58	38.50	35.84	33.52	31.49	29.70	28.09	26.65	25.35	24.17	23.10
0.30	62.36	58.28	54.70	51.54	48.72	46.19	43.92	41.85	39.97	38.25	36.68
0.40	83.15	78.44	74.24	70.47	67.06	63.96	61.14	58.56	56.18	53.99	51.96
0.50	103.90	98.95	94.45	90.34	86.58	83.12	79.92	76.96	74.21	71.65	69.26
0.60	124.70	119.90	115.46	111.33	107.50	103.91	100.56	97.42	94.46	91.69	89.07
0.70	145.50	141.26	137.26	133.48	129.91	126.52	123.30	120.24	117.33	114.56	111.92
0.80	166.30	163.03	159.90	156.88	153.98	151.18	148.48	145.87	143.36	140.93	138.58
0.90	187.10	185.24	183.43	181.65	179.90	178.19	176.50	174.85	173.24	171.65	170.09
1.00	207.90	207.88	207.88	207.88	207.88	207.88	207.88	207.88	207.88	207.88	207.88

Table 4 is provided as a supplement to Figure 25. It is worth noting that the information presented in both Figure 25 and Table 4 has been normalized with respect to the lateral area $\underline{A}_1$ of the clutch. Also, the concentric sphere assumption is meant to imply that the surrounding is capable of "seeing" all the clutch area, $\underline{A}_1$. Any obstruction or mounting will reduce the rate of radiant energy transfer.

Equation (5.16) is a result based upon assumptions about both the thermal characteristics of the clutch and surroundings and their relative configuration. The degree of accuracy attainable from this expression is totally dependent upon the way in which it is applied to any particular system. The accuracy of the calculation can be increased by improving the mathematical description of the configuration and/or by improving the data available on the thermal characteristics. The former is, in general, most difficult; the latter is more feasible and will here be discussed.

The gray-body assumption implies that the radiating body is radiating energy whose quantity is some fraction of that of an ideal black-body at the same temperature. This fractional quantity is the emissivity ϵ. The energy being radiated by a single gray-body can then be written in terms of the Stefan-Boltzmann law as

$$E_g = \varepsilon \sigma \bar{T}^4 \qquad (5.17)$$

Equation (5.17) may also be expressed by use of Planck's law, in terms of the wavelength of the radiation,

$$E_g = \varepsilon \int_0^\infty \frac{C_1 (\lambda)^{-5}}{\text{Exp}\ (C_2/\lambda \bar{T}) - 1}\, d\lambda \quad , \qquad (5.18)$$

where

E_g = emissive power of the gray-body
ε = emissivity of the gray-body
λ = wavelength of radiant emission
C_1 = 1.1870×10^4 BTU-μ^4/ft^2-hr
C_2 = 2.5896×10^4 ^oR-μ

The emissivity of any real surface is in general a function of both the wavelength and the temperature. In addition, the real surface may emit very nearly all its energy in a certain range of wavelengths. In this case the emissivity exclusive of this emitting range may be assumed zero.

Figure 26 shows a typical emissivity curve for an anodized aluminum surface. This curve is strictly applicable to a body at a temperature of 80^{o}F. However, the change in emissivity with a moderate temperature change is not appreciable. Hence, the application of this monochromatic emissivity to the case of the clutch and surrounding appear reasonable. It is now suggested that result (5.16) could be

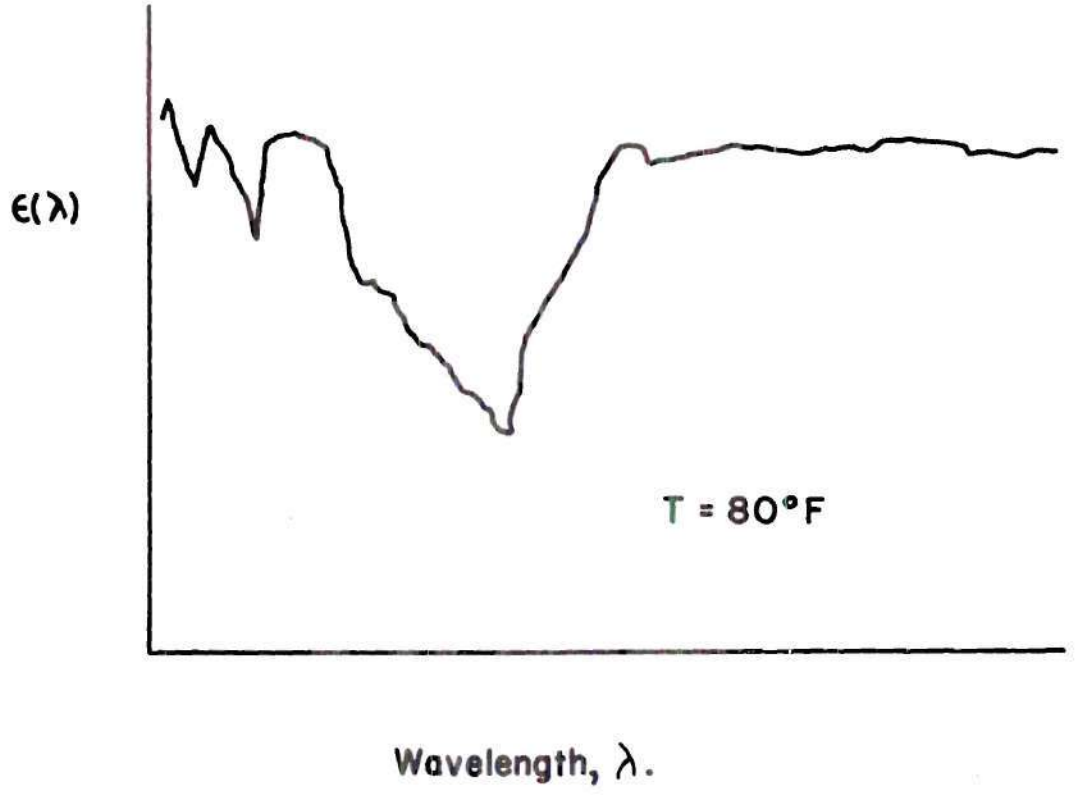

Figure 26. Monochromatic Emissivity of Anodized Aluminum Surface (Giedt (34))

modified for improved accuracy by the use of equation (5.18) and the additional information of Figure 26 to be

$$q = \frac{Q}{A_1} = \int_0^\infty \frac{\epsilon(\lambda)\left[E_1(\lambda,\bar{T}_1) - E_2(\lambda,\bar{T}_2)\right]}{1 + \left[1 - \epsilon(\lambda)\right]\frac{A_1}{A_2}}\, d\lambda \qquad (5.19)$$

where

$$\epsilon = \epsilon(\lambda) \qquad (5.20)$$

$$E_1(\lambda,\bar{T}_1) = \frac{C_1(\lambda)^{-5}}{\text{Exp}\ (C_2/\lambda\bar{T}_1) - 1} \qquad (5.21)$$

$$E_2(\lambda,T_2) = \frac{C_1(\lambda)^{-5}}{\text{Exp}\ (C_2/\lambda\bar{T}_2) - 1} \qquad (5.22)$$

Jakob (35) discusses several modifications of equations (5.16) and (5.19) which account for an asymmetric geometry and additional effects of irradiation.

Dissipative Energy of Typical Clutch Cycle

The energy to be dissipated from the clutch in any given cyclic operation is totally dependent upon the type of operation the clutch must accomplish. A particular example is discussed below.

The clutch will be assumed to be at a steady-state temperature throughout its operation. The energy W_d which must be dissipated during one cycle is necessarily the sum

of the energy, W_c, developed in the coils of the clutch and the energy, W_s, developed by slippage.

Assume that the clutch is required to transmit torque for t_a seconds. Then the coil current as a function of time will appear as shown in Figure 27 (a). The energy developed by the clutch coil is in general,*

$$W_c = \int_0^{t_a} RI^2(t)\, dt \qquad (5.23)$$

The actual form for I(t) during the cycle will greatly depend upon the type of electrical power source. If the actuation circuit is similar to that shown in Figure 13, the current can be represented as

$$I(t) = \begin{cases} K(1 - e^{-t/\tau}) & 0 \le t \le t_1 \\ I_{ss} & t_1 < t \le t_a \end{cases} \qquad (5.24)$$

Substituting equation (5.24) into (5.23) and integrating

$$W_c = K^2 \left[t_1 - 2\tau \left(1 - e^{-t_1/\tau}\right) + \tau/2 \left(1 - e^{-2t_1/\tau}\right) \right] + I_{ss}^2 R \left(t_a - t_1\right) \qquad (5.25)$$

If the system configuration is similar to that shown in Figure 1, an additional $I_q^2\, R(t_1)$ energy term must be considered with those shown in (5.25). This results from the fact that a small amount of current, I_q must be maintained

*Scott (36).

in the driven clutch in order to eliminate backlash.

The energy generated in the clutch as a result of slippage is the integral with respect to time of the product of slip torque and slip-speed. These quantities are shown in Figures 27 (a) and (c), respectively. Figure 27 (c) assumes that $\omega_1(t_a)$ is equal to $\omega_2(t_a)$ where subscripts "1" and "2" refer to input and output, respectively. Hence, the slip energy to be dissipated is given by

$$W_s = \int_0^{ta} T(t) \left[\omega_1(t) - \omega_2(t)\right] dt \qquad (5.26)$$

The total energy added to the clutch during a single engagement is

$$W_d = \int_0^{ta} RI^2(t)dt + \int_0^{ta} T(t) \left[\omega_1(t) - \omega_2(t)\right] dt \qquad (5.27)$$

Minimization of Dissipative Energy

Expression (5.27) is a general expression for the energy that must be dissipated per cycle to prevent the steady-state temperature of the clutch from rising. There is only one way in which the designer may minimize equation (5.27). That is, by the proper choice of clutch-torque level and load inertia. Figure 27 shows a typical engagement cycle in which the clutch-torque has achieved its steady-state

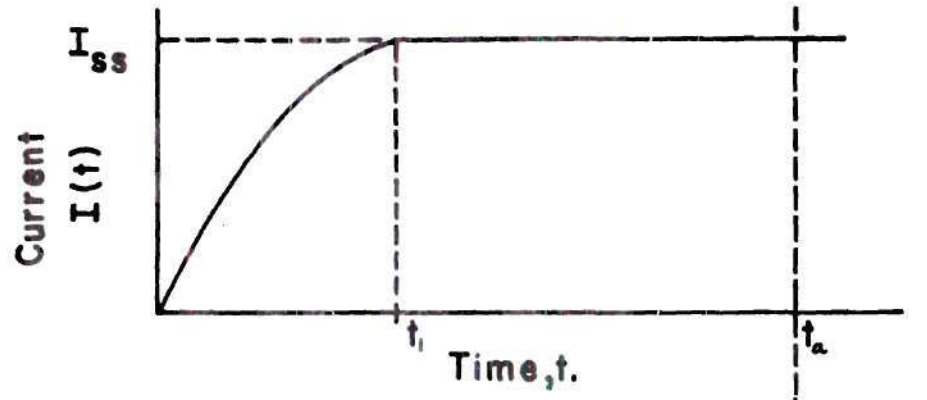

a) Current Time History

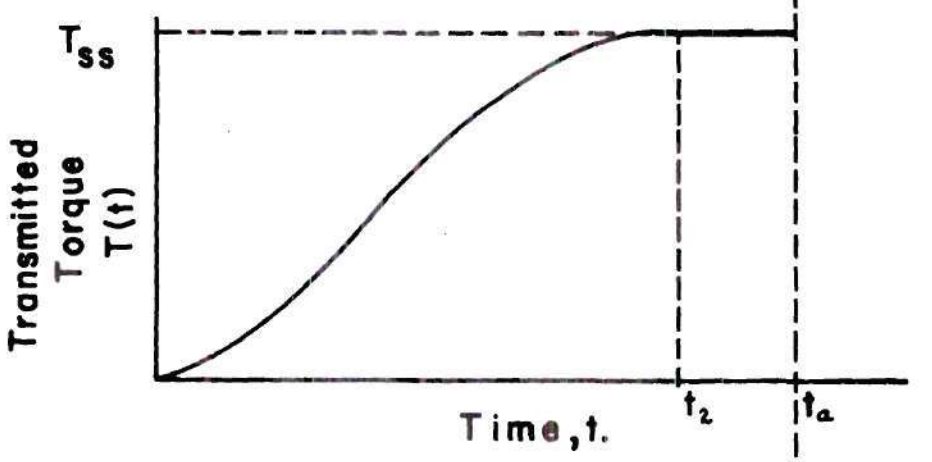

b) Transmitted Torque Time History

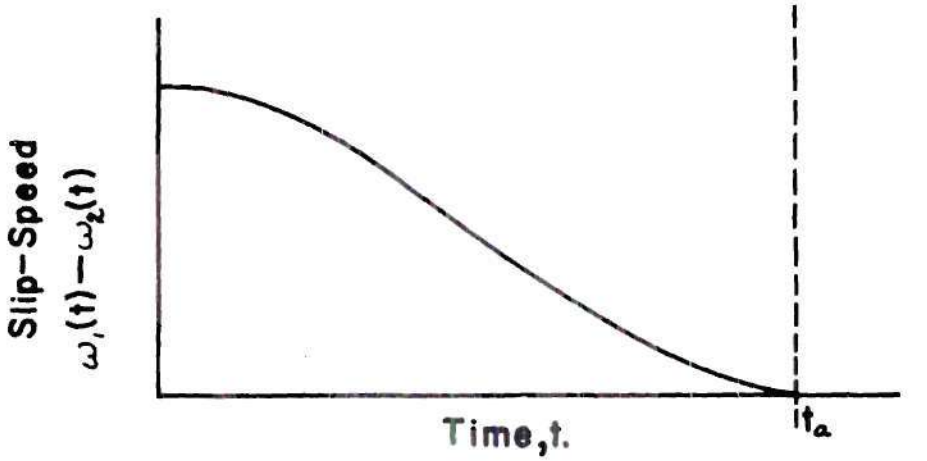

c) Slip-Speed Time History

Figure 27. Clutch Characteristics During Typical Engagement

level while the load is still experiencing acceleration (i.e., slip-speed does not equal zero). In general, it is best to eliminate clutch slippage after the clutch has attained its steady-state torque level, T_{ss}, (i.e., $t_a = t_2$). The possible exception is when the clutch must perform not only in its normal capacity as a torque transmitting device but also as a torque limiting device.

Assume that the load the clutch is driving is solely inertial in nature. Then, in order to minimize the dissipative energy of the clutch during one cycle, it is necessary to determine what steady-state torque level the clutch must be capable of achieving such that the load inertia has attained velocity ω_1 at time t_a. This will be done by calculating J_L, the load inertia, in terms of the steady-state torque level, T_{ss}. From this expression T_{ss} will be calculated in terms of the load inertia, J_L.

Since the load is purely inertial all the energy transmitted by the clutch to the output shaft must be equal to the change in kinetic energy of the output or load inertia, J_L. That is,

$$\tfrac{1}{2}J_L \left[\omega_2^2(t_a) - \omega_2^2(0)\right] = \int_0^{ta} T(t)\ \omega_2(t)dt \qquad (5.28)$$

But,

$$\omega_2(t_a) = \omega_1 \tag{5.29}$$

and, solving for J_L,

$$J_L = \frac{2}{\omega_1^2} \int_0^{ta} T(t) \quad \omega_2(t)\ dt + \frac{\omega_2^2(0)}{\omega_1^2} \tag{5.30}$$

It is also known that

$$T(t) = J_L \frac{d\omega_2(t)}{dt} \tag{5.31}$$

Or,

$$\omega_2(t) - \omega_2(0) = \frac{1}{J_L} \int_0^t T(t)\ dt \tag{5.32}$$

Solving expression (5.32) for $\omega_2(t)$ and using the dummy variable ξ, substitute into equation (5.30) to obtain equation (5.33).

$$J_L = \frac{2}{J_L \omega_1^2} \int_0^{ta} \int_0^{\xi} T(\xi)\ T(t) dt d\xi + \frac{2\omega_2(0)}{1^2} \int_0^{ta} T(\xi) d\xi + \frac{\omega_2^2(0)}{\omega_1^2} \tag{5.33}$$

Solving equation (5.33) for the load inertia, J_L,

$$J_L = \frac{\omega_2^2(0)}{2\omega_1^2} + \frac{\omega_2(0)}{\omega_1^2} \int_0^{ta} T(\xi)\ d\xi + \left[\left(\frac{\omega_2^2(0)}{2\omega_1^2} + \frac{\omega_2(0)}{\omega_1^2} \right. \right. \int_0^{ta} T(\xi) d\xi \Big)^2 + \frac{2}{\omega_1^2} \int_0^{ta} \int_0^{\xi} \left. \left. T(\xi) T(t) dt d\xi \right] \right]^{\frac{1}{2}} \tag{5.34}$$

In general, the evaluation of (5.34) is not simple. However, if functional information is available about the torque time history it is possible to derive meaningful results in a straight forward manner.

For example, assume that T(t) can be approximated by a straight line.* That is,

$$T(t) = kt \qquad 0 \leq t \leq t_a \tag{5.35}$$

Also, for simplicity let $\omega_2(0) = 0$. Then equation (5.34) becomes

$$J_L = \left[\frac{2}{\omega_1^2} \int_0^{ta} \int_0^{\xi} (k\xi)\ (kt)\ dt\ d\xi \right]^{\frac{1}{2}}$$

or,

$$J_L = \frac{kt_a^2}{2\omega_1} \tag{5.36}$$

But, it should be noted that $\underline{T}_{ss}$ is identically equal to $\underline{kt}_a$, hence,

$$T_{ss} = \frac{2\omega_1 J_L}{t_a} \tag{5.37}$$

Therefore, subject to the aforementioned assumptions and restrictions, equation (5.37) will establish the steady-

*Anderson (1) shows that this is the case for mechanical contact clutches.

state torque level required of a clutch to accelerate an inertia, J_L, from a velocity of zero to that of ω_1 in time t_a.

Result (5.27) is the amount of energy dissipated in the clutch during the engagement period t_a. The time period for one complete cycle is necessarily larger than t_a. It is an easy matter to relate the maximum cyclic frequency, N_{max} (cycles/unit time) to the energy dissipation characteristics of the clutch as

$$N_{max} = \frac{Q}{W_d} \quad . \tag{5.38}$$

In order to evaluate equation (5.38) it is first necessary to evaluate equation (5.16) and solve for Q explicitly. Then knowing the characteristics of the clutching cycle, equation (5.27) can be evaluated and hence N_{max} is determined.

CHAPTER VI

CONCLUSIONS

Electro-magnetic flux clutches and clutch couplings offer a variety of characteristics which may lend themselves to a space application. The electro-magnetic flux clutches have basically one control parameter, namely the coil current. This is in contrast to mechanical contact clutches which may be affected by friction coefficients, coil current and possibly lubrication. Hydraulic couplings are dependent upon both temperature and slip speed.

The electro-magnetic flux clutch coupling, commonly referred to as an eddy-current clutch, is capable of transmitting extremely high amounts of power. However, its means of operation requires that slippage occur to transmit torque. This necessarily requires additional energy dissipation over and above that encountered by any similar clutch. Since in any space application, heat transfer can be accomplished only by radiation or conduction, energy dissipation becomes a prime design consideration.

The magnetic-particle clutch is characterized by an extremely smooth operating cycle. Also, it is capable of

maintaining a constant torque even when subjected to 100 per cent slip. The magnetic-particle test clutches did not appear to have any hysteresis or eddy-current coupling effects. This would indicate a high degree of repeatability.

The steady-state and time varying relationship between torque and control current was found to be extremely non-linear. This added complexity does not lend itself to ready mathematical analysis, but various methods have been found and are documented. It was experimentally determined that when initially activated the dry-particle clutch may have an erratic torque characteristic as a result of an uneven particle distribution. However, this effect is minimized in most applications as a result of clutch motions. Only when the clutch is required to operate in a static "holding" mode may this phenomenon become predominant.

Finally, clutch temperature was found to affect noticeably the control coil resistance. However, it is not felt that this is a serious problem. An easy means of eliminating this situation is to use a temperature compensating resistor in conjunction with the clutch. Temperature did not measurably affect the torque-producing characteristics of the particle dust in the working gap.

The hysteresis clutch was found to display all the

characteristics of the magnetic-particle clutch exclusive of those dependent upon the magnetic-particle dust. In general, the hysteresis clutch is more bulky than the magnetic-particle and in consequence of its means of operation is much heavier in weight.

Also, the asynchronous or hysteresis clutch has an extremely slow rise time; taking as much as three times as long as the comparable particle clutch to attain full engagement. However, a compensating characteristic is its smoothness of operation. In this respect the hysteresis clutch excels above all other designs.

It is concluded that electro-magnetic flux clutches are quite applicable to space designs. The electro-magnetic flux clutch-coupling is not considered a useful device in these specialized applications since it will encounter excessive temperature. Finally, these clutches may prove most applicable in designs requiring extreme repeatability, long periods of slip operation and the complete absence of in-service adjustments.

APPENDIX A

INSTRUMENTATION AND EQUIPMENT

Figure 11 shows a block diagram of the experimental system used in this investigation. The components comprising the system may be considered to perform one of three functions. These are hydraulic drive, feedback or control and instrumentation.

Hydraulic Drive Apparatus

The prime mover of the system was a Vickers hydraulic motor, Model AR-10007-BEL. Hydraulic fluid at a pressure of 750 pounds per square inch was supplied by a Denison "HydrOILic" pumping unit. A Moog, Model 22-135A, electrically actuated servo-valve provided a precise control of fluid to and from the hydraulic motor. The capacity of the servo-valve limited the range of velocities available for testing. For this reason, a "by-pass" was provided to increase the total volumetric flow rate to the motor. Precise velocity control was still maintained through the servo-valve.

In order to reduce the effects of engaging the test

clutch on the drive line a large inertia flywheel was mounted immediately after the prime mover. The mass inertia of the flywheel was 35.381 (in.-lb-sec^2). Figure 28 shows a schematic of the hydraulic drive system.

Feedback and Control

Velocity control was obtained by tachometer feedback. A Fairchild Industries, model 532-Al, d.c. generator was geared to the output shaft of the flywheel through a 60:112 gear ratio. The total gain from flywheel shaft to generator output was 0.00357 volts per revolution per minute (volts/rpm). The field voltage of the generator was externally maintained at 12 volts d.c. through the use of the silicon diode power supply shown in Figure 29.

The output of the generator was found to contain some high frequency noise. To eliminate this a low-pass filter was designed. The transfer function for the filter was

$$\frac{E_{out}(s)}{E_{in}(s)} = \frac{\tau_1 s + 1}{\tau_2 s + 1} = \frac{0.000156s+1}{0.016 s+1} \quad \text{(A-1)}$$

A circuit diagram is shown in Figure 30(a).

The summing circuit was constructed of simple resistances. Also, the inversion of the generator output was accomplished in the summing circuit. The error voltage used

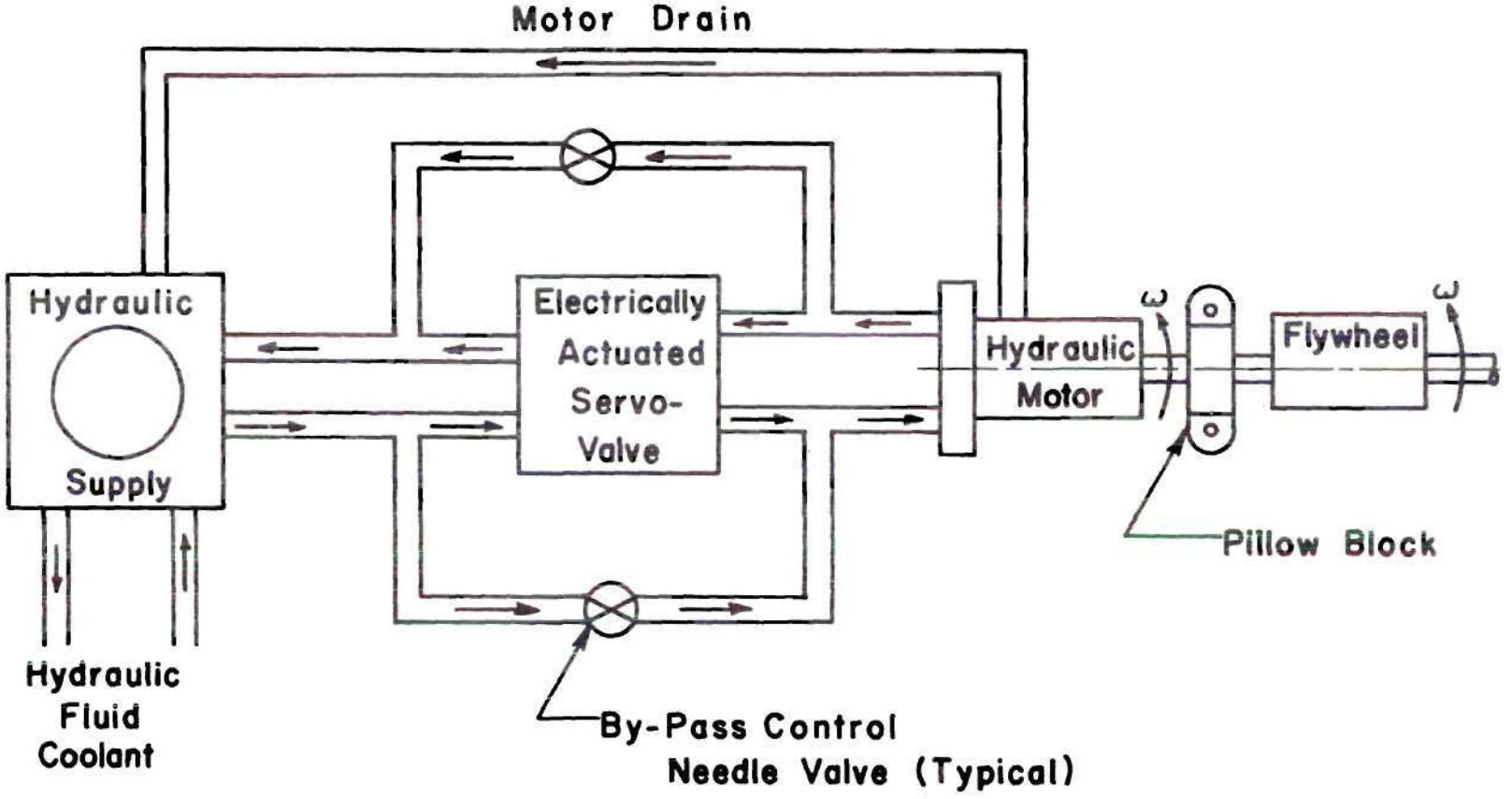

Figure 28. Hydraulic Drive System

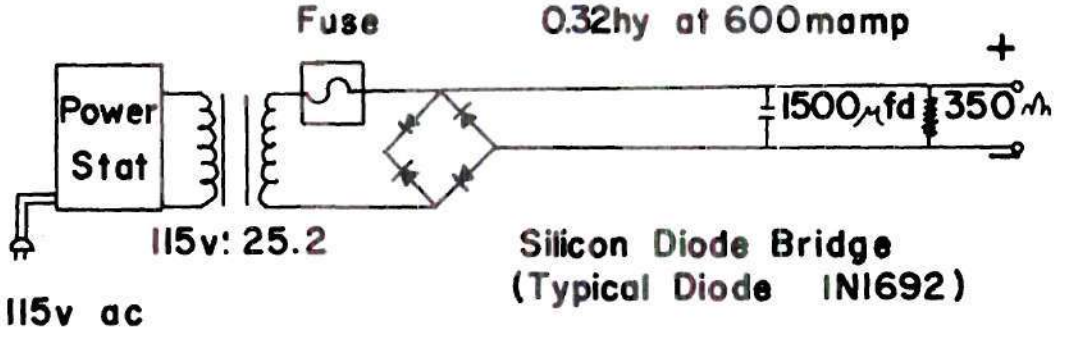

Figure 29. Silicon Diode Power Supply for Tachometer Field Voltage

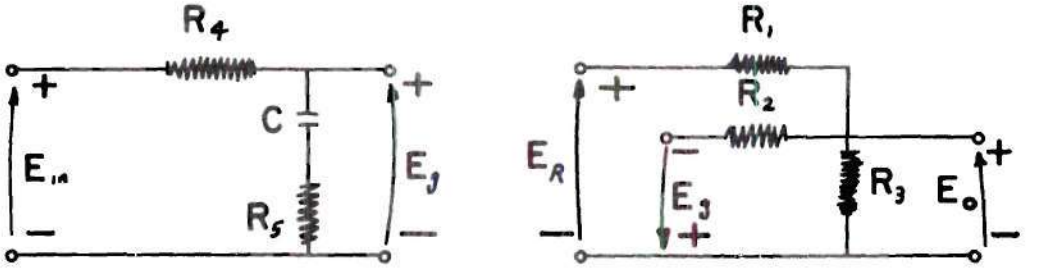

$$\frac{E_o}{E_i} = \frac{\tau_1 s + 1}{\tau_2 s + 1} = \frac{0.000156\,s + 1}{0.016\,s + 1}$$

$$E_o = \frac{R_3(R_2 E_R - R_1 E_g)}{R_1 R_2 + R_1 R_3 + R_2 R_3}$$

a) Generator Output Filter

$$\cong \frac{E_R - E_g}{12}$$

b) Summing Circuit

Figure 30. Feed-back and Control Components

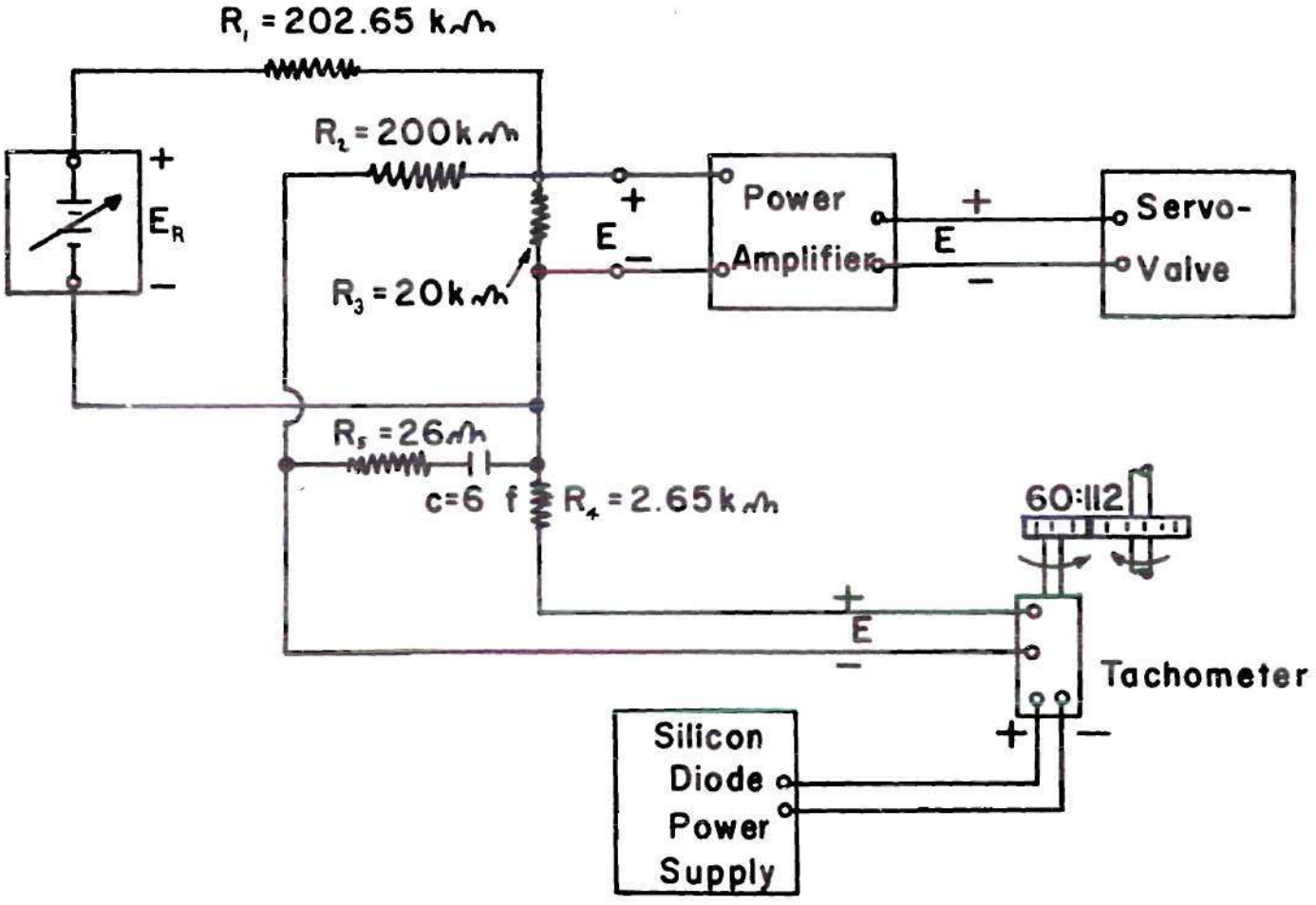

Figure 31. Schematic Diagram of Feedback and Control System

to control the servo-valve was related to the reference voltage and generator filter output by equation (A-2).

$$E_{out} = \frac{R_3(R_2E_r - R_1E_g)}{R_1R_2 + R_1R_3 + R_2R_3} \quad \frac{E_r - E_g}{12} \qquad \text{(A-2)}$$

E_o = error voltage
E_r = reference voltage
E_g = generator filter output

The reference voltage was obtained from a Harrison Laboratories, model 6204A, d.c. power supply with vernier output control. The error voltage was fed to the servo-valve through a Dymec, model 2460A, amplifier.

Figure 31 shows a schematic of the feedback and control systems.

Instrumentation

A visual monitor was maintained on the velocity of the main drive shaft of the apparatus. A spur gear with 120 teeth was mounted on the flywheel shaft. A Power Instruments, model 836, photosensitive pickup was arranged such that a pulse was generated as each tooth of the spur gear passed the photosensor. The output of the sensor was sampled by an Hewlett-Packard 52331 electronic counter for periods of one second. The count displayed by the counter was then twice the speed of the shaft in revolutions per minute.

The torque transmitted by the test clutch was measured by a Lebow strain gauge bridge torque transducer. The model 1214-100 with a maximum torque capability of 200 inch-pounds was used for the larger clutches. The smaller clutches were tested with the model MTE-200 having a 200 inch-ounce capability.

The output of the torque transducer was amplified and recorded in a Sanborn model 350-1100B dual channel strip chart recorder. One channel was used to record the torque transducer output, the second was used to indicate when the clutch current was initiated. A one ohm resistor was placed in series with the clutch coil. The voltage across this resistor was used to determine the current through the clutch coil. This voltage was recorded on a Textronic Type 564 Storage Oscilloscope equipped with a Type 3172 dual-trace amplifier.

It was also possible to record the torque transducer output on the oscilloscope. For this purpose the transducer output was amplified in the Sanborn pre-amplifier, filtered through a low-pass filter and finally recorded on the oscilloscope. The scope sweep was initiated by the clutch actuation circuit.

APPENDIX B

EXPERIMENTAL DATA

The following is a presentation of the data collected on the clutches investigated in the laboratory. Each clutch is signified by its manufacturer's code letter and clutch model code number.

Each clutch displayed similar time response data, with one important exception. Clutches I-4, I-5 and I-8 are magnetic-particle clutches. Clutch D-4 is an hysteresis clutch. The magnetic-particle clutches displayed a slightly different time response for various slip-speeds and coil currents. This was not the case with the hysteresis clutch. This difference in performance was solely a result of the particle distribution in the working gap of the particle clutches. As the hysteresis clutch had no working medium it was not subject to these results.

One additional test was performed. This was to ascertain the effect of hysteresis and eddy-current coupling as explained in Chapter IV. Each clutch was subjected to all tests at the same time. Each clutch was periodically tested to see that its steady-state response had remained constant.

This was the case and hence no hysteresis effects were measurable. Also, each clutch was engaged at a constant torque level and then subjected to its maximum speed at 100 per cent slip. No variation in torque was noticeable indicating a lack of eddy-current coupling.

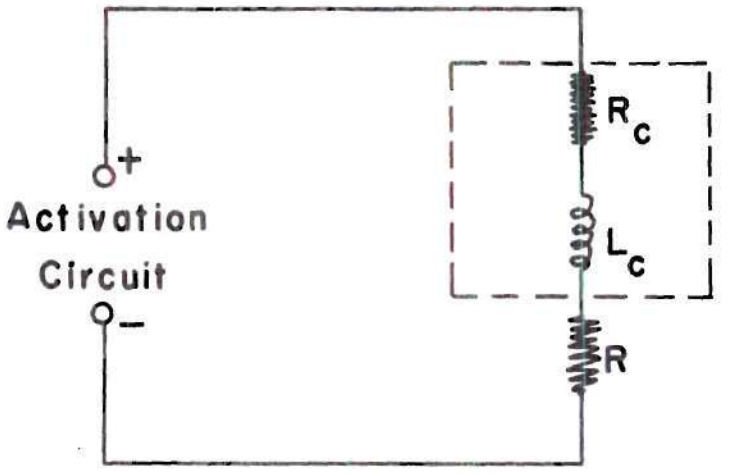

Figure 32. Circuit Diagram for Actuation of Clutch I-5

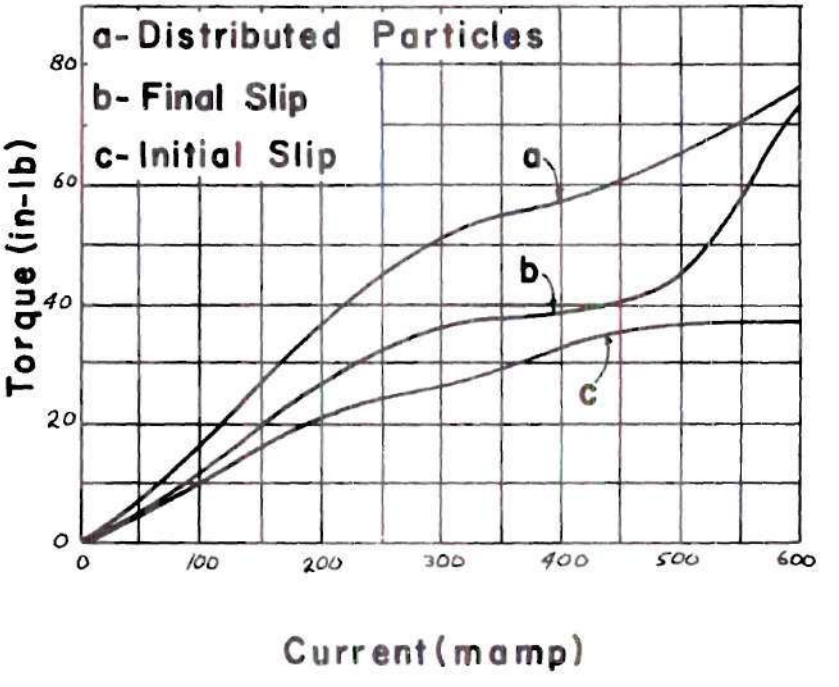

Figure 33. Static Slip Torque vs. Current for Clutch I-5

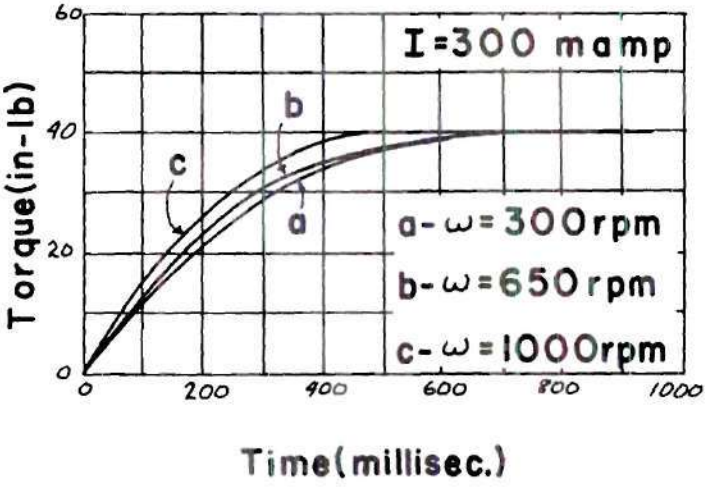

Figure 34. Torque Build-up at Various Slip-Speeds for Clutch I-5

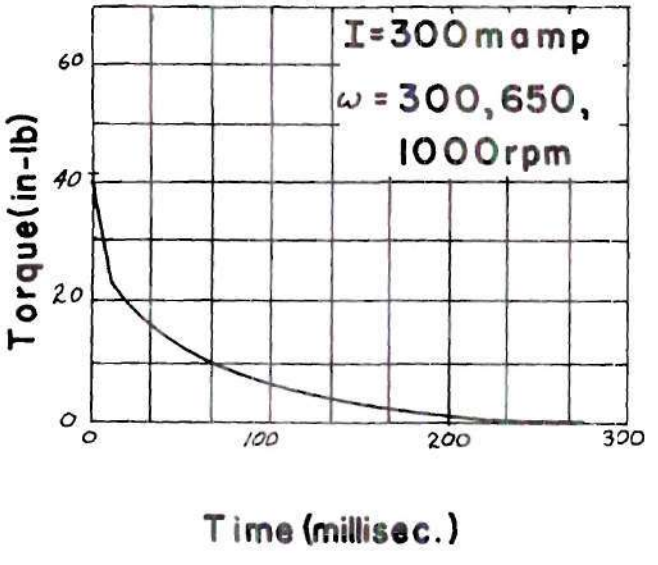

Figure 35. Torque Decay at Various Slip-Speeds for Clutch I-5

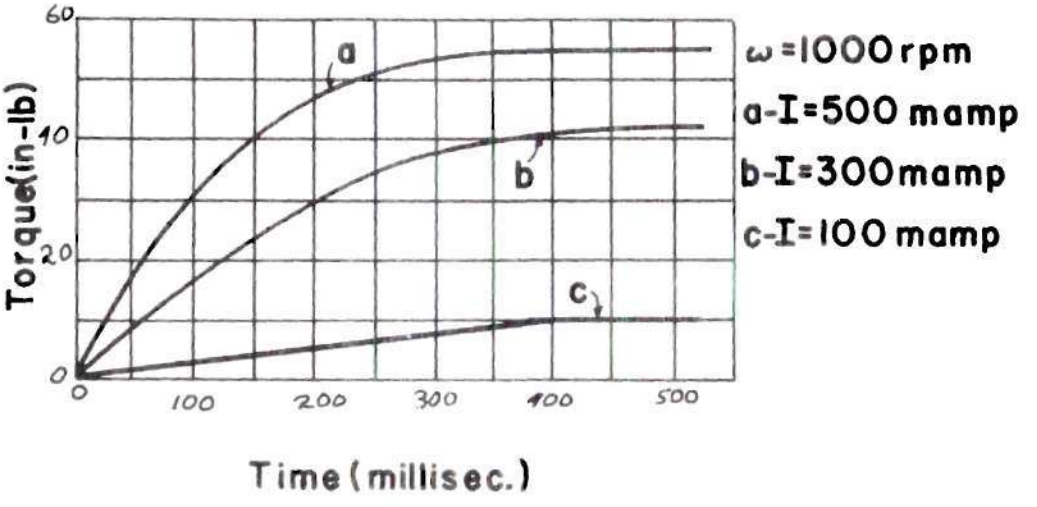

Figure 36. Torque Build-up as a Function of Steady-State Current Level for Clutch I-5

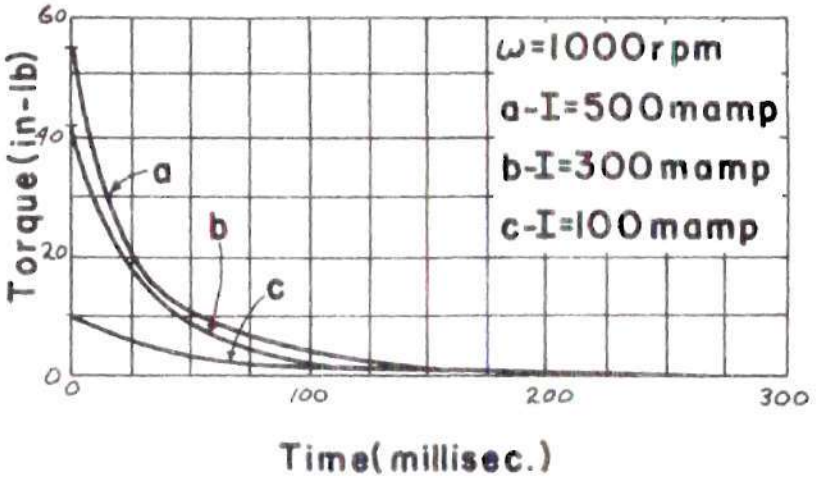

Figure 37. Torque Decay as a Function of Steady-State Current Level for Clutch I-5

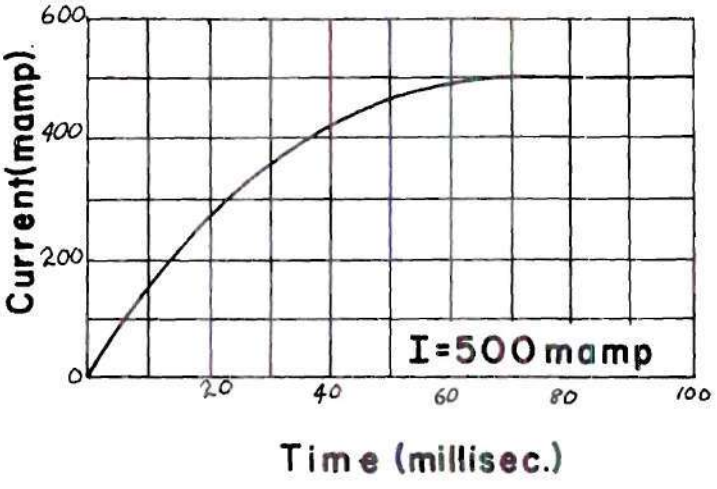

Figure 38. Current Build-up with Normal Activation Circuit for Clutch I-5

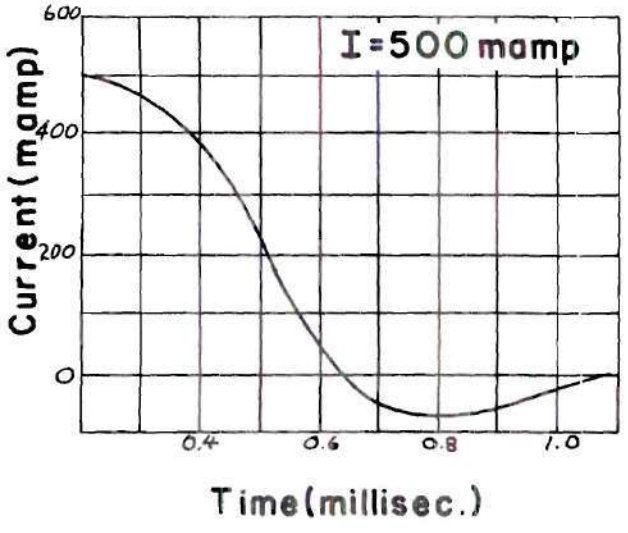

Figure 39. Current Decay with Normal Activation Circuit for Clutch I-5

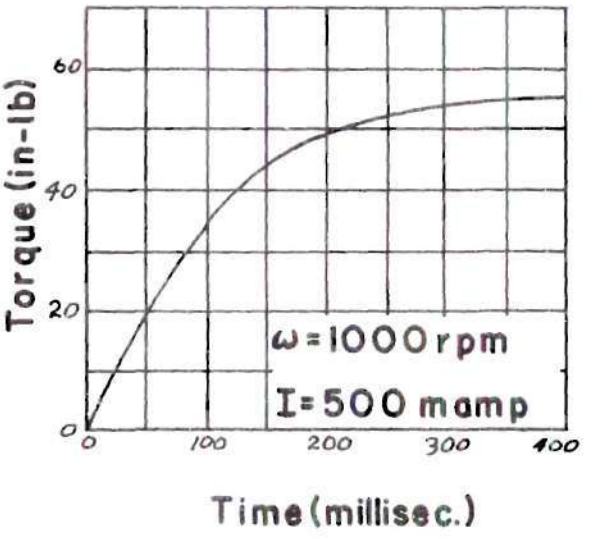

Figure 40. Torque Build-up with Special Activation Circuit for Clutch I-5

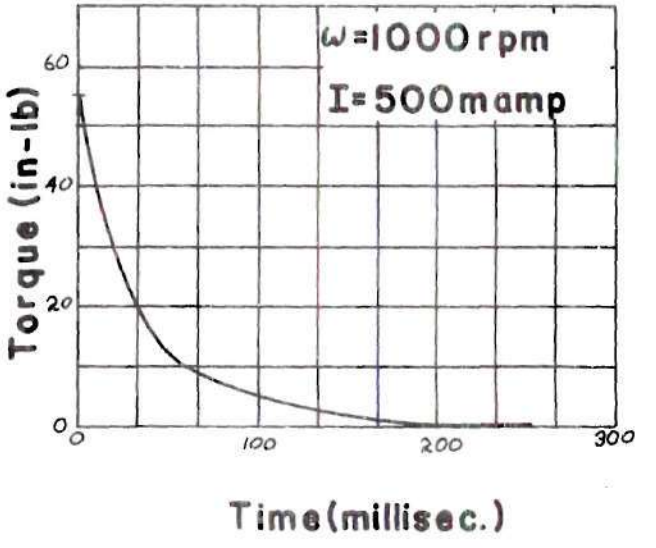

Figure 41. Torque Decay with Special Activation Circuit for Clutch I-5

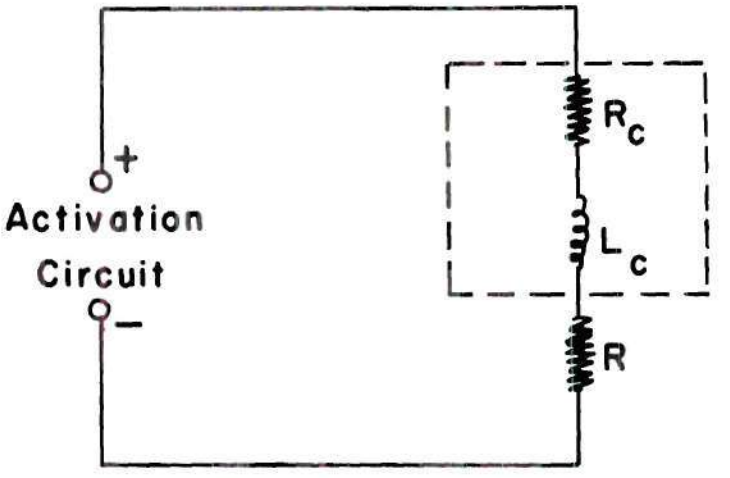

Figure 42. Circuit Diagram for Actuation of Clutch D-4

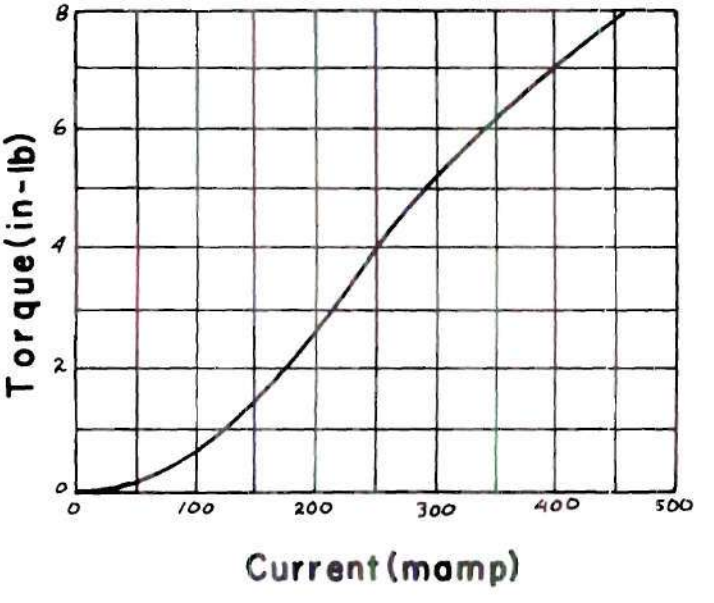

Figure 43. Static Slip Torque vs. Current For Clutch D-4

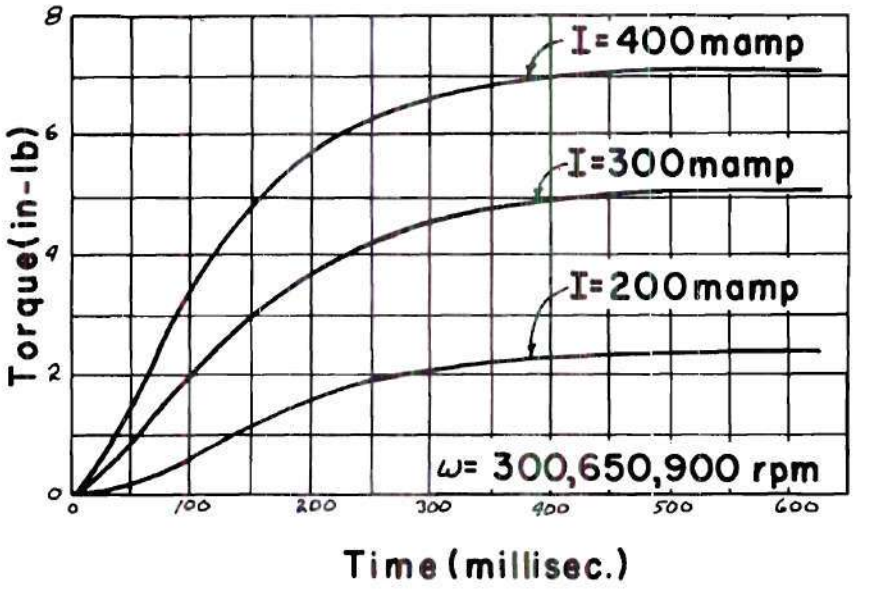

Figure 44. Torque Build-up as a Function of Current Level and Slip-Speed for Clutch D-4

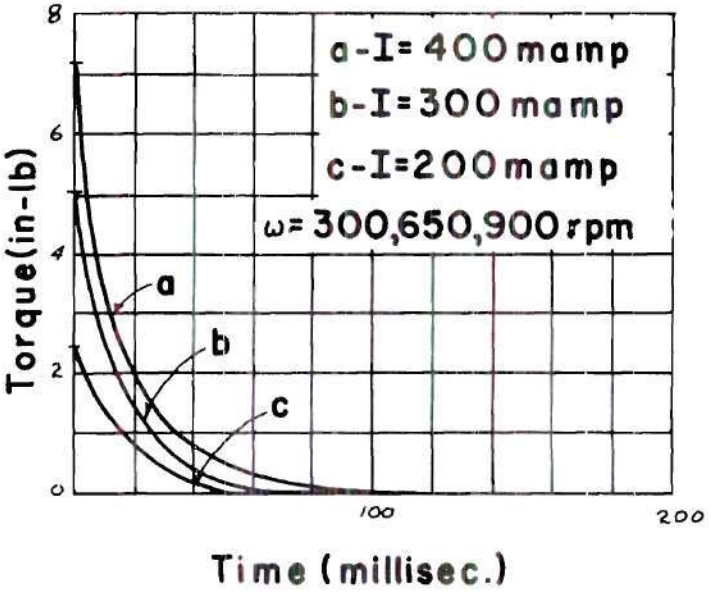

Figure 45. Torque Decay as a Function of Current Level and Slip-Speed for Clutch D-4

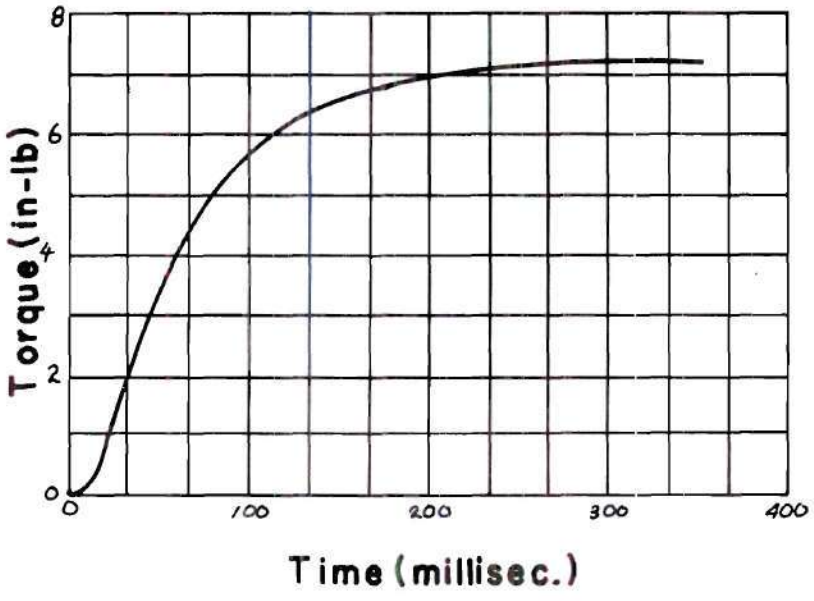

Figure 46. Torque Build-up with Special Activation Circuit for Clutch D-4

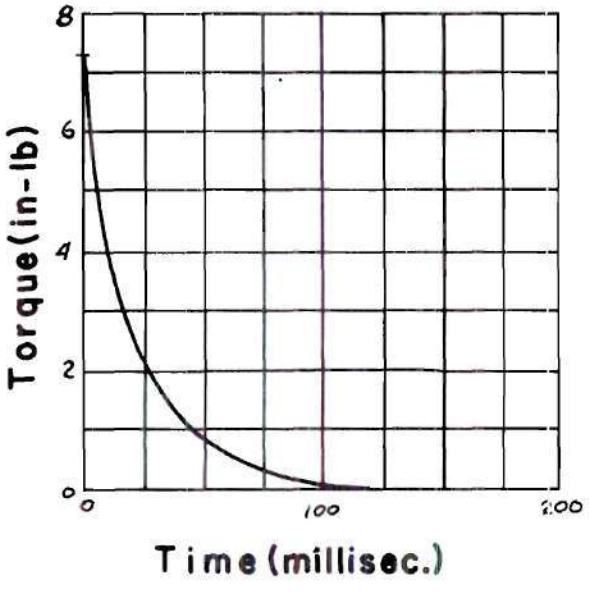

Figure 47. Torque Decay with Special Activation Circuit for Clutch D-4

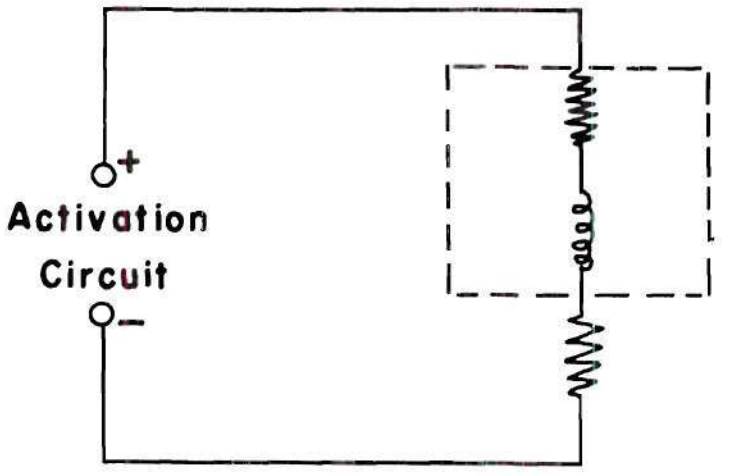

Figure 48. Circuit Diagram for Actuation of Clutch I-8

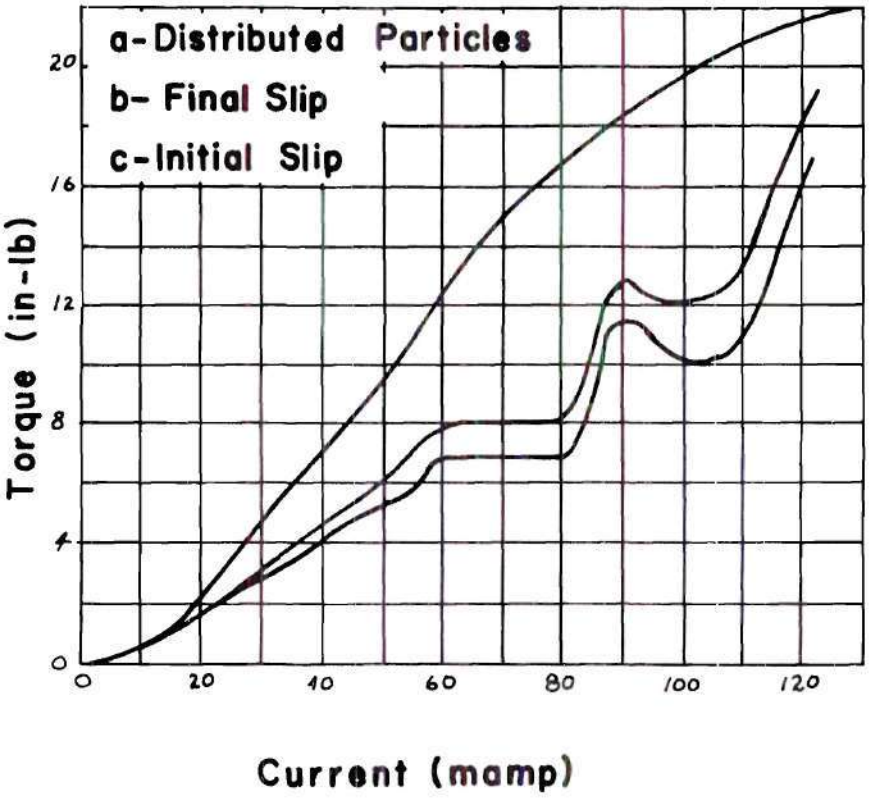

Figure 49. Static Slip Torque vs. Current for Clutch I-8

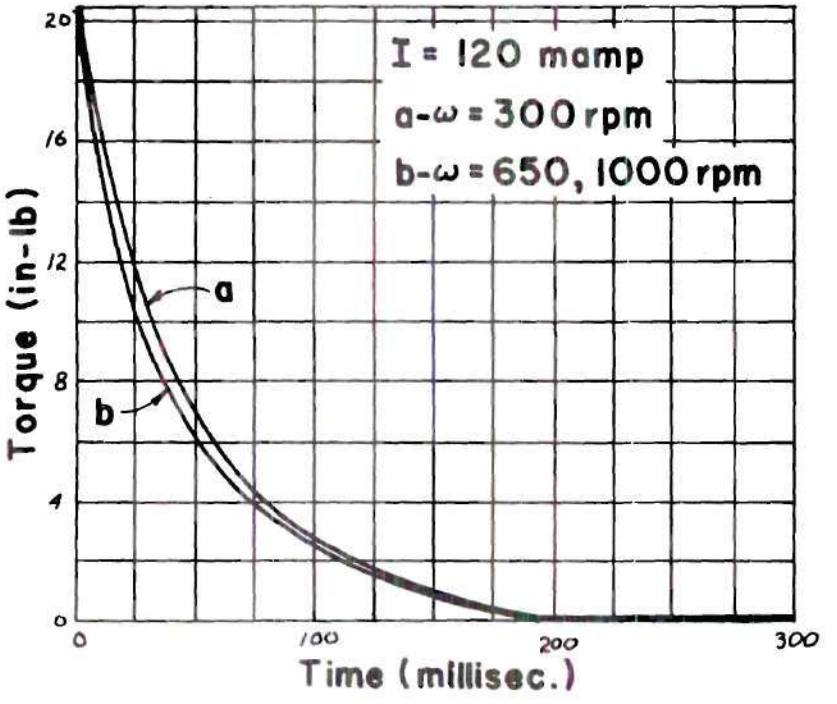

Figure 50. Torque Decay at Various Slip-Speeds for Clutch I-8

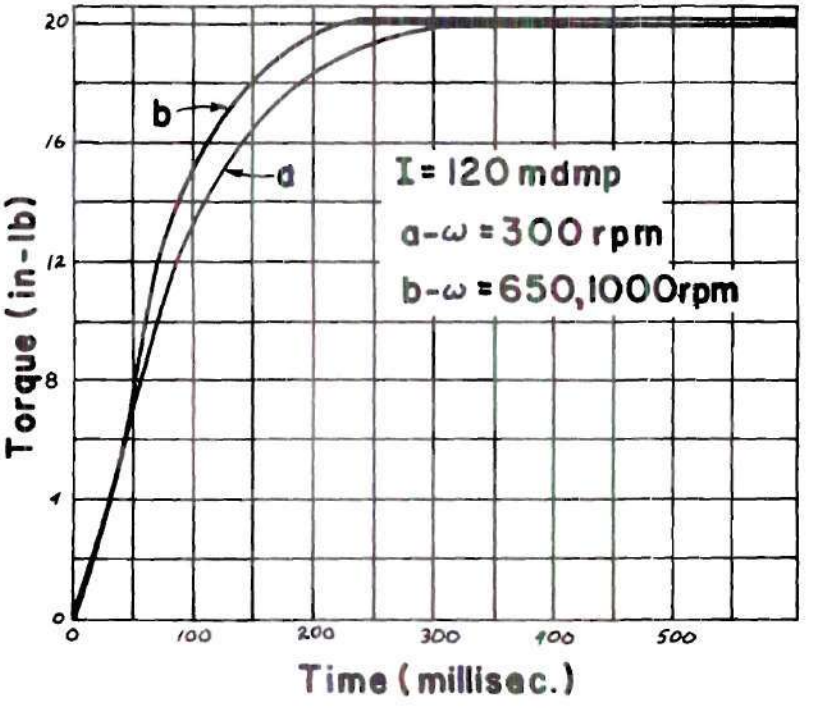

Figure 51. Torque Build-up at Various Slip-Speeds for Clutch I-8

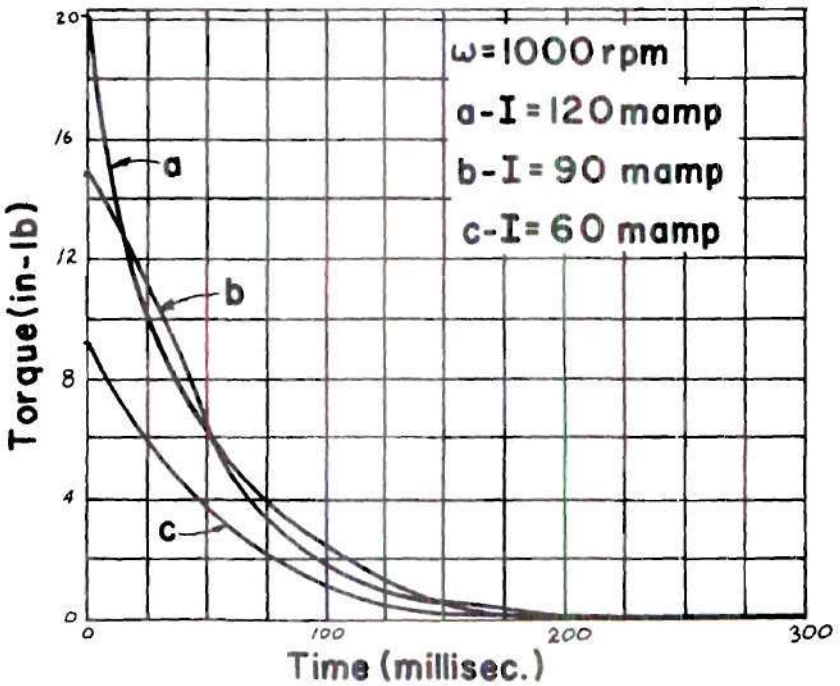

Figure 52. Torque Decay as a Function of Current Level for Clutch I-8

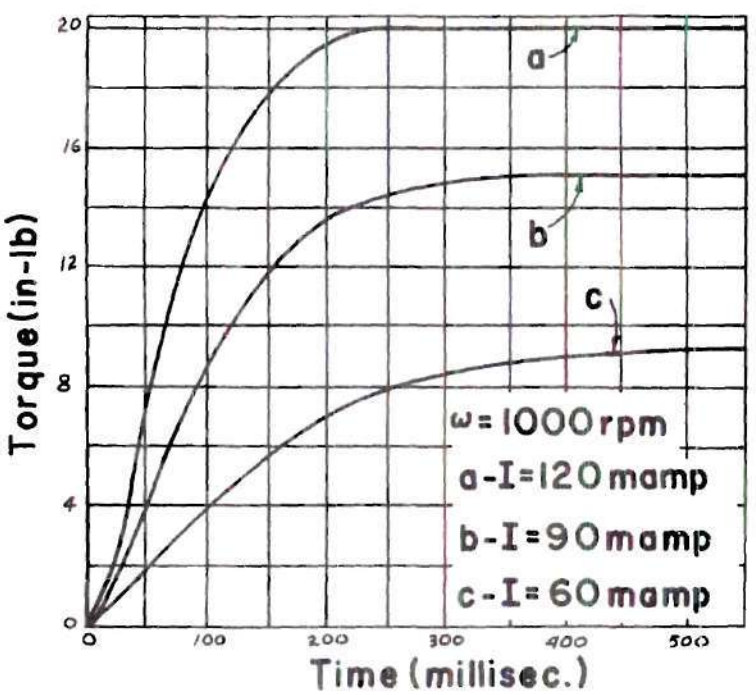

Figure 53. Torque Build-up as a Function of Current Level for Clutch I-8

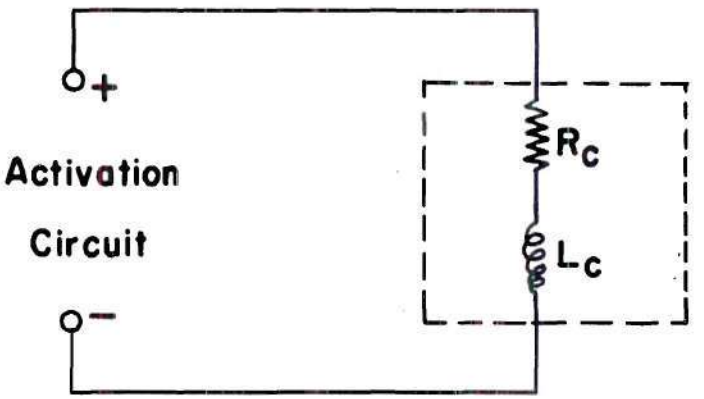

Figure 54. Circuit Diagram for Actuation of Clutch I-4

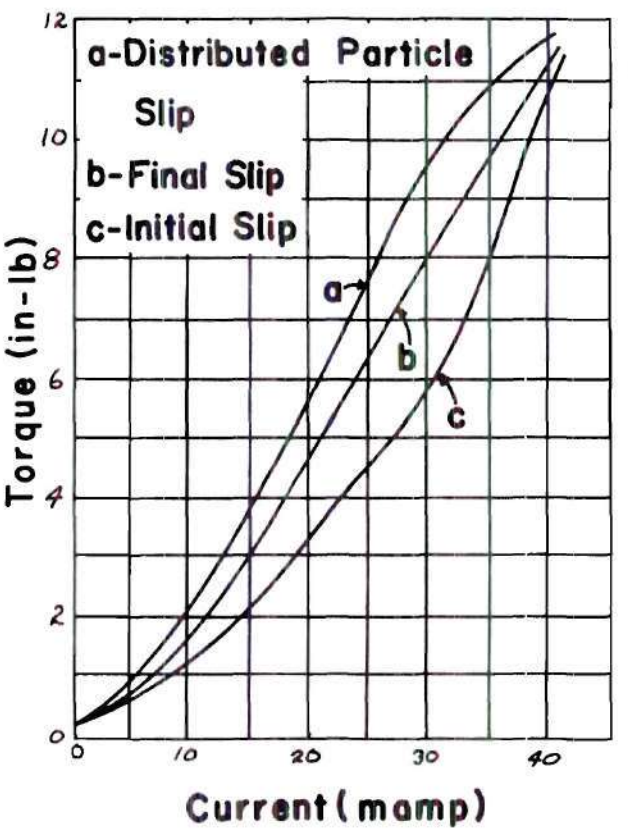

Figure 55. Static Slip Torque vs. Current for Clutch I-4

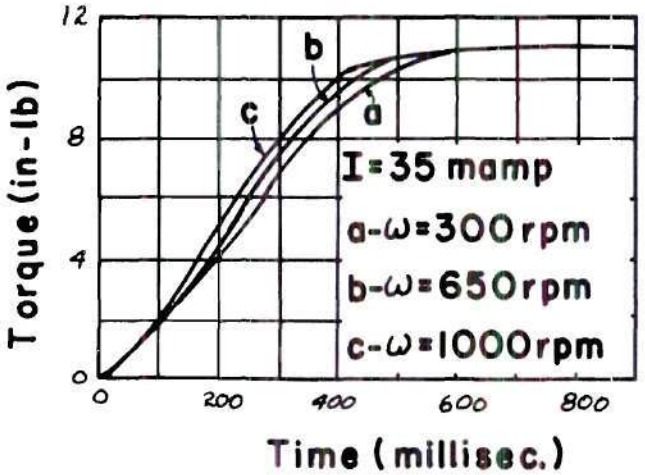

Figure 56. Torque Build-up at Various Slip-Speeds for Clutch I-4

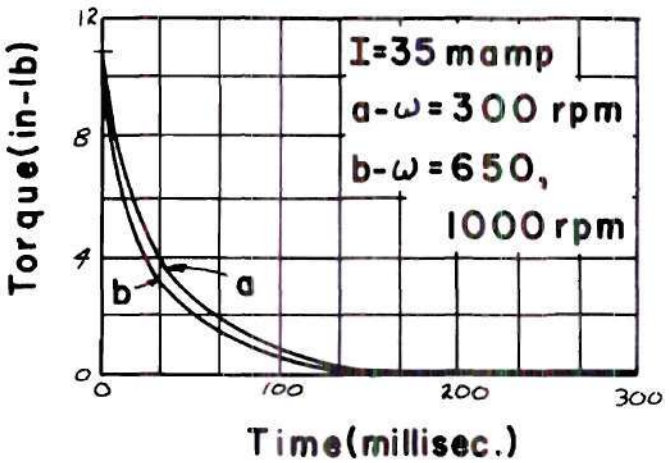

Figure 57. Torque Decay at Various Slip-Speeds for Clutch I-4

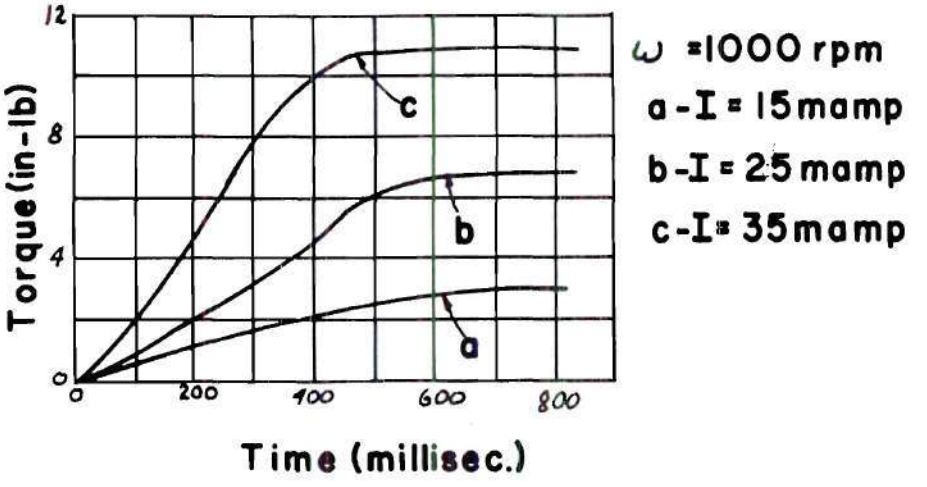

Figure 58. Torque Build-up as a Function of Current Level for Clutch I-4

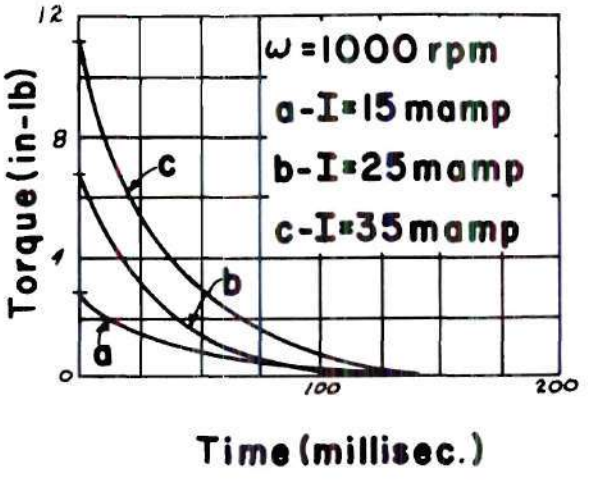

Figure 59. Torque Decay as a Function of Current Level for Clutch I-4

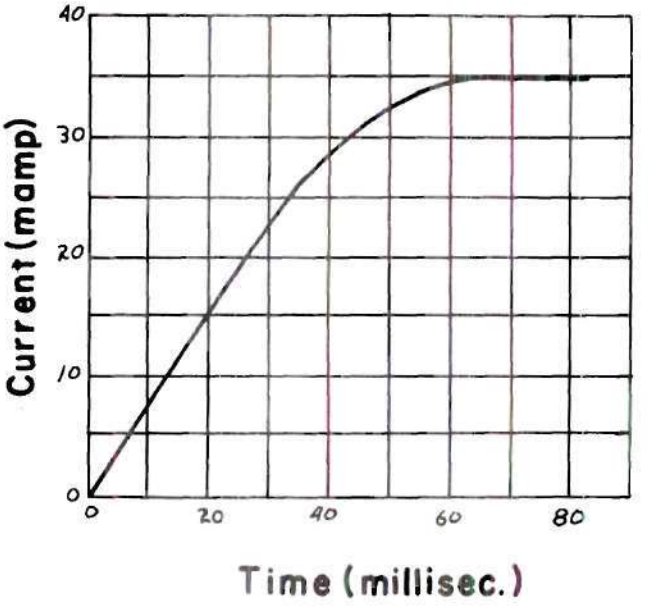

Figure 60. Current Build-up with Normal Activation Circuit for Clutch I-4

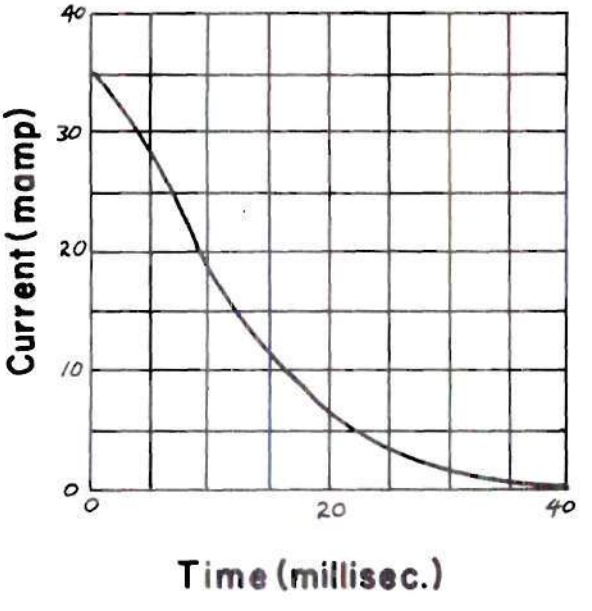

Figure 61. Current Decay with Normal Activation Circuit for Clutch I-4

APPENDIX C

CLUTCH MANUFACTURERS

Table 5 and Table 6 are a key to the clutch manufacturers and clutch models considered in this investigation. The typical clutches tested in the experimental portion of this study were I-4, I-5, I-8, and D-4.

Table 5. Key to Clutch Manufacturers

Code Letter	Manufacturer's Name
A	General Electro-Mechanical Corporation Buffalo, New York
B	American Precision Industries, Inc. Buffalo, New York
C	Dynamic Instrument Corporation Plainview, Long Island, New York
D	Magtrol, Inc. Buffalo, New York
E	Vickers, Inc. Electric Products Division St. Louis, Missouri
F	F A E Instrument Corporation Huntington Station, New York
G	SEC'S, Inc. Long Island City, New York
H	Vibrac, Corporation Chelmsford, Massachusetts
I	Lear-Siegler, Inc. Electro-Mechanical Division Grand Rapids, Michigan

Table 6. Key to Clutch Manufacturers' Clutch Models

Clutch Code Number / Manufacturer Code Letter	A	B	C	D	E	F	G	H	I
1	PMC-6-1	HYC-20	HFC-2.5	HCS-160	32D103	F-160	CX42	5CC-1-1	3538B
2	PMC-16-1	HYC-30	HFC-6.0	HCS-200	32D161			8C-1-1	892C
3	PMC-30-1	HYC-35	HFC-16.0	HCS-300	32D101			11C-1-2	890A
4	PMC-35-1	HYC-40	HFC-32.0	HCS-500	32D145			15C-1-2	900AB
5	PMC-120-1	HYC-45	HFC-110	HC-100	32D98			16C-1-1	878B
6	PMC-175-1	HYC-50	HFC-200	HC-200				23C-1-1	917L
7	PMC-350-1	HYC-55	HFC-350	HC-300					909
8		FHYC-30		HC-500					3500C
9		FHYC-45		HC-600					
10		FHYC-55		HC-700					

BIBLIOGRAPHY

1. R. I. Anderson, Mechanical-Contact Clutches for Space Applications, Master's Thesis, Georgia Institute of Technology, February, 1966.

2. W. A. Jones, An Evaluation of Hydrodynamic Fluid Clutches for Space Applications, Master's Thesis, Georgia Institute of Technology, May, 1966.

3. J. Rabinow, "The Magnetic-Fluid Clutch," National Bureau of Standards, TR 1213.

4. J. Winston, "Design and Application of Hysteresis Clutches," Electrical Manufacturing, Vol. 60, December, 1957, pp. 114-127.

5. R. P. Bleikamp, "The Electromagnetic Drive . . . An Economical Answer to Many Drive Problems," Westinghouse Engineer, Vol. 20, May, 1960, pp. 71-75.

6. T. M. Vorob'yeva, Electromagnetic Clutches and Couplings, translated from Russian by O. M. Blunn and edited by A. D. Booth, Pergamon Press, 1965, pp. 148-151.

7. Ibid., pp. 60-85.

8. E. P. Blackburn, Jr., A Mathematical Model for a Dry Powdered Magnetic Clutch, Master's Thesis, University of California, Los Angeles, June, 1960.

9. "Mechanical Contact Clutches," Machine Design, Vol. 24, Pt. 2, August, 1952, pp. 125-158.

10. T. R. Stuelphagel and J. P. Dallas, "Consideration of Off-On-Modulated Clutch Servo Systems," AIEE Transactions, Vol. 71, Pt. 2, January, 1953, pp. 406-410.

11. J. Proctor, "Selecting Clutches for Mechanical Drives," Product Engineering, Vol. 32, Pt. 2, June 19, 1961, pp. 43-58.

12. S. A. Davis, "Miniature Magnetic Clutches and Brakes," Electromechanical Components and Systems Design, Vol. 8, January, 1964, pp. 129-138.

13. B. King, "Applying Electro-Magnetic Clutch Drives for Positioning Applications," Automation, Vol. 11, Pt. 1, March, 1964, pp. 56-58.

14. Vorob'yeva, pp. 138-143.

15. R. P. Bleikamp, "The Electro-Magnetic Drive," Machine Design, Vol. 32, Pt. 2, May 12, 1960, pp. 180-184.

16. R. S. Baker, "Design of an Eddy-Current Brake for a Sodium-Cooled Reactor," Electrical Engineering, Vol. 79, April, 1960, pp. 282-285.

17. D. Graham, "Magnetic Clutches Add Muscle to Electronic Servos," Space/Aeronautics, Vol. 31, April, 1959, pp. 1308-1315.

18. J. Rabinow, "The Magnetic Fluid Clutch," AIEE Transactions, Vol. 67, Pt. 2, 1948, pp. 1308-1315.

19. A. J. Parziale and P. D. Tilton, "Characteristics of Some Magnetic-Fluid Clutch Servo-Mechanisms," AIEE Transactions, Vol. 69, Pt. 1, 1950, pp. 150-157.

20. W. P. Jones, "Investigation of Magnetic Mixtures for Clutch Applications," AIEE Transactions, Vol. 72, Pt. 3, April, 1953, pp. 88-92.

21. "Ferromagnetic Coupling Development," The Engineer (London), Vol. 195, May 9, 1953, pp. 703-704.

22. R. Grau and B. A. Chubb, "The Magnetic Particle Clutch," Aerospace Engineering, Vol. 20, November, 1961, pp. 18-43.

23. G. M. Flidlider, "Transient Response in the Magnetic Circuits of Electro-Magnetic Clutches," Automation and Remote Control, Vol. 20, January, 1959, pp. 27-40.

24. P. N. Kopai-Gora, "Concerning Some Properties of Ferromagnetic Clutches," Automation and Remote Control, Vol. 19, 1948, pp. 361-369.

25. D. L. Swords, "Magnetic Clutches for Continuous Slip," Product Engineering, Vol. 32, Pt. 2, August 28, 1961, pp. 23-28.

26. J. S. Proctor, "How to Select Electro-Magnetic Clutches and Brakes for Automatic Control," Product Engineering, Vol. 32, Pt. 3, December 19, 1961, pp. 29-34.

27. S. Iatesta, "Realistic Ways to Speed Response of D. C. Clutches and Brakes," Product Engineering, Vol. 32, Pt. 1, January 23, 1961, pp. 41-44.

28. Anderson, pp. 6-8.

29. Anderson, pp. 42-49.

30. Blackburn, pp. 8-10.

31. T. A. Glasenko, "Some Problems in the Design of an Asynchronous Clutch with a Monolithic Rotor," Automation and Remote Control, Vol. 19, 1958, pp. 783-790.

32. J. D. Slocum, "A Method for the Determination of Temperature Rise Due to Slippage in Magnetic-Particle Clutches," GREM 106, Temperature Rise Test Program on Lear Magnetic-Particle Clutches, Par. 6.2.1., New Military Products, Blueprint for 1961.

33. F. Krieth, Principles of Heat Transfer, International Textbook Company, Scranton, Pennsylvania, 1962, pp. 175-232.

34. W. H. Giedt, Principles of Engineering Heat Transfer, D. Van Nostrand, Co., Inc., New York, 1957, pp. 231-274.

35. M. Jakob, Heat Transfer, Vol. II, John Wiley & Sons, Inc., New York, 1957, pp. 1-89.

36. R. E. Scott, Linear Circuits, Part I, Addison-Wesley Publishing Co., Reading, Massachusetts, 1960, pp. 192-259.

37. R. W. Young, Report on Metal Powder Industries Federation, 15th Annual Meeting, April, 1959, Pt. 2, pp. 113-119.